Article

C#F Activation of Fluorinated Arenes using NHC-Stabilized Nickel(0) Complexes: Selectivity and Mechanistic Investigations

Thomas Schaub, Peter Fischer, Andreas Steffen, Thomas Braun, Udo Radius, and Andreas Mix

J. Am. Chem. Soc., **2008**, 130 (29), 9304-9317 • DOI: 10.1021/ja074640e • Publication Date (Web): 28 June 2008

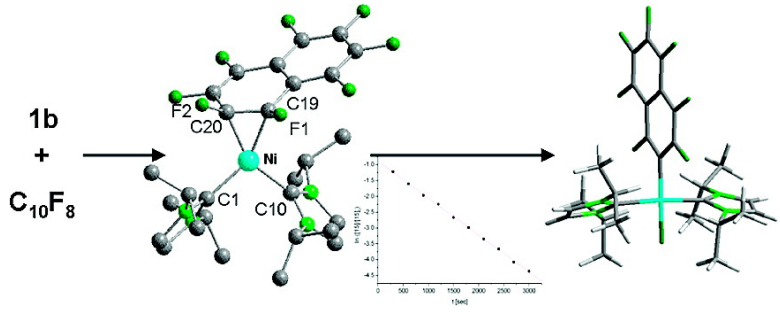

More About This Article

Additional resources and features associated with this article are available within the HTML version:

- Supporting Information
- Links to the 4 articles that cite this article, as of the time of this article download
- Access to high resolution figures
- Links to articles and content related to this article
- Copyright permission to reproduce figures and/or text from this article

View the Full Text HTML

J|A|C|S
ARTICLES

Published on Web 06/28/2008

C−F Activation of Fluorinated Arenes using NHC-Stabilized Nickel(0) Complexes: Selectivity and Mechanistic Investigations

Thomas Schaub,[†] Peter Fischer,[†] Andreas Steffen,[‡] Thomas Braun,*[,‡] Udo Radius,*[,†] and Andreas Mix[§]

Institut für Anorganische Chemie der Universität Karlsruhe, 76131 Karlsruhe, Germany, Institut für Chemie, Humboldt-Universität zu Berlin, Brook-Taylor-Strasse 2, 12489 Berlin, Germany, and Fakultät für Chemie, Universität Bielefeld, Universitätsstrasse 25, 33615 Bielefeld, Germany

Received June 25, 2007; E-mail: thomas.braun@chemie.hu-berlin.de; radius@aoc1.uni-karlsruhe.de

Abstract: The reaction of [Ni_2(^{i}Pr$_2$Im)$_4$(COD)] **1a** or [Ni(^{i}Pr$_2$Im)$_2$(η^2-C_2H_4)] **1b** with different fluorinated arenes is reported. These reactions occur with a high chemo- and regioselectivity. In the case of polyfluorinated aromatics of the type C_6F_5X such as hexafluorobenzene (X = F) octafluorotoluene (X = CF_3), trimethyl(pentafluorophenyl)silane (X = $SiMe_3$), or decafluorobiphenyl (X = C_6F_5) the C−F activation regioselectively takes place at the C−F bond in the *para* position to the X group to afford the complexes *trans*-[Ni(^{i}Pr$_2$Im)$_2$(F)(C_6F_5)] **2**, *trans*-[Ni(^{i}Pr$_2$Im)$_2$(F)(4-(CF_3)C_6F_4)] **3**, *trans*-[Ni(^{i}Pr$_2$Im)$_2$(F)(4-(C_6F_5)C_6F_4)] **4**, and *trans*-[Ni(^{i}Pr$_2$Im)$_2$(F)(4-($SiMe_3$)C_6F_4)] **5**. Complex **5** was structurally characterized by X-ray diffraction. The reaction of **1a** with partially fluorinated aromatic substrates $C_6H_xF_y$ leads to the products of a C−F activation *trans*-[Ni(^{i}Pr$_2$Im)$_2$(F)(2-C_6FH_4)] **7**, *trans*-[Ni(^{i}Pr$_2$Im)$_2$(F)(3,5-$C_6F_2H_3$)] **8**, *trans*-[Ni(^{i}Pr$_2$Im)$_2$(F)(2,3-$C_6F_2H_3$)] **9a** and *trans*-[Ni(^{i}Pr$_2$Im)$_2$(F)(2,6-$C_6F_2H_3$)] **9b**, *trans*-[Ni(^{i}Pr$_2$Im)$_2$(F)(2,5-$C_6F_2H_3$)] **10**, and *trans*-[Ni(^{i}Pr$_2$Im)$_2$(F)(2,3,5,6- C_6F_4H)] **11**. The reaction of **1a** with octafluoronaphthalene yields exclusively *trans*-[Ni(^{i}Pr$_2$Im)$_2$(F)(1,3,4,5,6,7,8-$C_{10}F_7$)] **6a**, the product of an insertion into the C−F bond in the 2-position, whereas for the reaction of **1b** with octafluoronaphthalene the two isomers *trans*-[Ni(^{i}Pr$_2$Im)$_2$(F)(1,3,4,5,6,7,8-$C_{10}F_7$)] **6a** and *trans*-[Ni(^{i}Pr$_2$Im)$_2$(F)(2,3,4,5,6,7,8-$C_{10}F_7$)] **6b** are formed in a ratio of 11:1. The reaction of **1a** or of **1b** with pentafluoropyridine at low temperatures affords *trans*-[Ni(^{i}Pr$_2$Im)$_2$(F)(4-C_5NF_4)] **12a** as the sole product, whereas the reaction of **1b** performed at room temperature leads to the generation of *trans*-[Ni(^{i}Pr$_2$Im)$_2$(F)(4-C_5NF_4)] **12a** and *trans*-[Ni(^{i}Pr$_2$Im)$_2$(F)(2-C_5NF_4)] **12b** in a ratio of approximately 1:2. The detection of intermediates as well as kinetic studies gives some insight into the mechanistic details for the activation of an aromatic carbon−fluorine bond at the {Ni(^{i}Pr$_2$Im)$_2$} complex fragment. The intermediates of the reaction of **1b** with hexafluorobenzene and octafluoronaphthalene, [Ni(^{i}Pr$_2$Im)$_2$(η^2-C_6F_6)] **13** and [Ni(^{i}Pr$_2$Im)$_2$(η^2-$C_{10}F_8$)] **14**, have been detected in solution. They convert into the C−F activation products. Complex **14** was structurally characterized by X-ray diffraction. The rates for the loss of **14** at different temperatures for the C−F activation of the coordinated naphthalene are first order and the estimated activation enthalpy $\Delta H^{\ddagger}$ for this process was determined to be $\Delta H^{\ddagger} = 116 \pm 8$ kJ mol^{-1} ($\Delta S^{\ddagger} = 37 \pm 25$ J K^{-1} mol^{-1}). Furthermore, density functional theory calculations on the reaction of **1a** with hexafluorobenzene, octafluoronaphthalene, octafluorotoluene, 1,2,4-trifluorobenzene, and 1,2,3-trifluorobenzene are presented.

Introduction

In the past few years there has been a growing interest in the transition metal mediated activation of carbon−fluorine bonds.[1] One major stimulation has been the demand for a stoichiometric and catalytic derivatization of highly fluorinated substrates via C−F activation and C−C coupling reactions at a transition metal center.[2–4] However, fundamental problems comprise questions

[†] Institut für Anorganische Chemie der Universität Karlsruhe.
[‡] Humboldt-Universität zu Berlin.
[§] Universität Bielefeld.

(1) (a) For reviews on C−F activation see : Doherty, N. M.; Hoffmann, N. W. *Chem. Rev.* **1991**, *91*, 553. (b) Burdeniuc, J.; Jedlicka, B.; Crabtree, R. H. *Chem. Ber./Recl.* **1997**, *130*, 145. (c) Kiplinger, J. L.; Richmond, T. G.; Osterberg, C. E. *Chem. Rev.* **1994**, *94*, 373. (d) Murphy, E. F.; Murugavel, R.; Roesky, H. W. *Chem. Rev.* **1997**, *97*, 3425. (e) Mazurek, U.; Schwarz, H. *Chem. Commun.* **2003**, 1321. (f) Braun, T.; Perutz, R. N. *Chem. Commun.* **2002**, 2749. (g) Torrens, H. *Coord. Chem. Rev.* **2005**, *249*, 1957. (h) Jones, W. D. *Dalton Trans.* **2003**, 3991. (i) Perutz, R. N.; Braun, T. In *Comprehensive Organometallic Chemistry III*; Crabtree, R. H., Mingos M. P., Eds.; Elsevier: Oxford, England, 2007; Vol. 1, p 725.

(2) (a) Hughes, R. P.; Zhang, D.; Zakharov, L. N.; Rheingold, A. L. *Organometallics* **2002**, *21*, 4902. (b) Hughes, R. P.; Laritchev, R. B.; Zakharov, L. N.; Rheingold, A. L. *J. Am. Chem. Soc.* **2005**, *127*, 6325. (c) Fujiwara, M.; Ichikawa, J.; Okauchi, T.; Minami, T. *Tetrahedron Lett.* **1999**, *40*, 7261. (d) Terao, J.; Ikumi, A.; Kuniyasu, H.; Kambe, N. *J. Am. Chem. Soc.* **2003**, *125*, 5646. (e) Huang, Y. Z.; Li, J.; Zhou, J.; Zhu, Z.; Hou, G. *J. Organomet. Chem.* **1981**, *205*, 185. (f) Huang, Y. Z.; Li, J.; Zhou, J.; Wang, Q.; Gui, M. *J. Organomet. Chem.* **1981**, *218*, 169. (g) Edelbach, B. L.; Kraft, B. M.; Jones, W. D. *J. Am. Chem. Soc.* **1999**, *121*, 10327. (h) Braun, T.; Parsons, S.; Perutz, R. N.; Voith, M. *Organometallics* **1999**, *18*, 1710. (i) Noveski, D.; Braun, T.; Neumann, B.; Stammler, A.; Stammler, H.-G. *Dalton Trans* **2004**, 4106. (j) Deacon, G. B.; Koplick, A. J.; Raverty, W. D.; Vince, D. G. *J. Organomet. Chem.* **1979**, *182*, 121. (k) Braun, T.; Wehmeier, F.; Altenhöner, K. *Angew. Chem.* **2007**, *119*, 5415; *Angew. Chem., Int. Ed.* **2007**, *46*, 5321.

10.1021/ja074640e CCC: $40.75

on the chemo- and regioselectivity of carbon−fluorine bond cleavage reactions.[1,3,5] Selective transformations can often be a challenge, partly because of the strength of a C−F bond and/or the kinetic inertness of some systems toward C−F activation.[6] It is therefore of fundamental interest to gain a profound understanding of the mechanisms of C−F activation reactions in order to design new metal complexes showing activity toward the activation and functionalization of fluorocarbons.[1]

Several reaction pathways for the cleavage of a carbon−fluorine bond in fluoroaromatics have been discussed, one of which is a concerted oxidative addition, mostly found at d^{10} metals such as nickel, palladium, or platinum.[1,5,7] At nickel, the oxidative addition of hexafluorobenzene at the complex fragment $\{Ni(PEt)_2\}$ has been described by Fahey and Mahan in 1977.[8] The product *trans*-$[Ni(PEt_3)_2(F)(C_6F_5)]$ was isolated in low yields of 7%. Perutz and co-workers have published more detailed studies. They isolated the C−F activation product in moderate yields and reported a complete spectroscopic and crystallographic characterization.[5f] The formation of the C−F activation product requires several weeks to be complete. On using the bidentate chelating ligand $^tBu_2PC_2H_4P^tBu_2$, Pörschke et al. were able to isolate an intermediate, which exhibits an η^2-coordinated C_6F_6 ligand at the nickel center. The complex undergoes C−F activation to the cis product upon heating.[9] Perutz et al. also observed the η^2-coordination of octafluoronaphthalene at a $\{Ni(PEt_3)_2\}$ unit.[10] The complex converts thermally into *trans*-$[Ni(PEt_3)_2(F)(1,3,4,5,6,7,8\text{-}C_{10}F_7)]$. ^{19}F NMR spectroscopic investigations confirm the reaction rate to be of first order, which is compatible with an intramolecular concerted oxidative addition reaction pathway. The activation of fluorinated pyridines and pyrimidines at $\{Ni(PEt_3)_2\}$ has also been reported. The conversions exhibit an unusual chemoselectivity for C−F over C−H activation.[1f,5]

We recently reported the synthesis and characterization of the NHC (N-heterocyclic carbene) stabilized nickel complex $[Ni_2(^iPr_2Im)_4(COD)]$ **1a** ($^iPr_2Im$ =1,3-di(*iso*propyl)imidazol-2-ylidene), which is a source of the $\{Ni(^iPr_2Im)_2\}$ complex fragment in stoichiometric as well as in catalytic transformations.[11] Compound **1a** is an excellent catalyst for the insertion of diphenyl acetylene into the 2,2′-C−C bond of biphenylene, very efficient for the oxidative addition of a C−F bond of hexafluorobenzene or perfluorinated toluene and a suitable catalyst for Suzuki type C−C cross-coupling reactions of perfluorinated arenes with organic boronic acids.[11] In contrast to the activation reactions mentioned above, which require long reaction times, the oxidative addition at $[Ni_2(^iPr_2Im)_4(COD)]$ **1a** proceeds very fast at room temperature (see eq 1).[11] In this paper we give a detailed account on C−F activation reactions of fluorinated arenes using the complexes $[Ni_2(^iPr_2Im)_4(COD)]$ **1a** or $[Ni(^iPr_2Im)_2(\eta^2\text{-}C_2H_4)]$ **1b**. These reactions occur with a high chemo- and regioselectivity, and the detection of intermediates, kinetic studies as well as theoretical calculations give some insight into the mechanistic details for the activation of an aromatic carbon−fluorine bond at the $\{Ni(^iPr_2Im)_2\}$ complex fragment.

Results

C−F Activation of Fluorinated Aromatics. The reaction of **1a** with stoichiometric amounts of C_6F_6 in benzene or toluene proceeds fast and smoothly at room temperature.[11a,c] The oxidative addition of one of the C−F bonds of hexafluorobenzene is completed within one hour at room temperature leading to the yellow reaction product *trans*-$[Ni(^iPr_2Im)_2(F)(C_6F_5)]$ **2** in good isolated yield (see eq 1). The reaction is quantitative according to the NMR data of the reaction mixture. Treatment of $[Ni(^iPr_2Im)_2(\eta^2\text{-}C_2H_4)]$ **1b** and hexafluorobenzene also affords complex **2** in good yield, although the reaction appears to be slower. Moreover, **2** is available in a one-pot procedure in approximately 50% isolated yield starting from $[Ni(COD)_2]$, the carbene, and hexafluorobenzene.

In the ^{19}F NMR spectrum of **2**, three signals at −116.0, −163.3, and −165.0 ppm were detected for the perfluorinated phenyl ligand, and, most significantly, a resonance was detected at a high magnetic field of −373.7 ppm for the fluoro ligand.

(3) (a) Braun, T.; Perutz, R. N.; Sladek, M. I. *Chem. Commun.* **2001**, 2254. (b) Steffen, A.; Sladek, M. I.; Braun, T.; Neumann, B.; Stammler, H.-G. *Organometallics* **2005**, *24*, 4057. (c) Braun, T.; Izundu, J.; Steffen, A.; Neumann, B.; Stammler, H.-G. *Dalton Trans.* **2006**, 5118. (d) Braun, T.; Noveski, D.; Ahijado, M.; Wehmeier, F. *Dalton Trans.* **2007**, 3820.

(4) (a) For catalytic cross-coupling reactions by C−F activation of monofluorinated arenes see: Kiso, Y.; Tamao, K.; Kumada, M. *J. Organomet. Chem.* **1973**, *50*, C12. (b) Böhm, V. P. W.; Gstöttmayr, C. W. K.; Weskamp, T.; Herrmann, W. A. *Angew. Chem,* **2001**, *113*, 3500; *Angew. Chem., Int. Ed*. **2001**, *40*, 2287. (c) Widdowson, D. A.; Wilhelm, R. *Chem. Commun.* **1999**, 2211. (d) Wilhelm, R.; Widdowson, D. A. *J. Chem. Soc., Perkin Trans.* **2000**, *1*, 3808. (e) Kim, Y. M.; Yu, S. *J. Am. Chem. Soc.* **2003**, *125*, 1696. (f) Mongin, F.; Mojovic, L.; Giullamet, B.; Trécourt, F.; Quéguiner, G. *J. Org. Chem.* **2002**, *67*, 8991. (g) Widdowson, D. A.; Wilhelm, R. *Chem. Commun.* **2003**, 578. (h) Dankwardt, J. E. *J. Organomet. Chem.* **2005**, *690*, 932. (i) Lamm, K.; Stollenz, M.; Meier, M.; Görls, H.; Walter, D. *J. Organomet. Chem.* **2003**, *681*, 24. (j) Bahmanyar, S.; Borer, B. C.; Kim, Y. M.; Kurtz, D. M.; Yu, S. *Org. Lett.* **2005**, *7*, 1011. (k) Terao, J.; Watabe, H.; Kambe, N. *J. Am. Chem. Soc.* **2005**, *127*, 3656. (l) Saeki, T.; Y.; Takashima, Y.; Tamao, K. *Synlett* **2005**, 1771. (m) Ackermann, L.; Born, R.; Spatz, J. H.; Meyer, D. *Angew. Chem.* **2005**, *117*, 7382; *Angew Chem., Int. Ed.* **2005**, *44*, 7216. (n) Korn, T. J.; Schade, M. A.; Knochel, P. *Org. Lett.* **2006**, 725. (o) Guo, H.; Kong, F.; Kanno, K.; He, J.; Nakajima, K.; Takahashi, T. *Organometallics* **2006**, *25*, 2045. (p) Wang, T.; Alfonso, B. J.; Love, J. A. *Org. Lett.* **2007**, *9*, 5629.

(5) (a) Jasim, N. A.; Perutz, R. N.; Whitwood, A. C.; Braun, T.; Izundu, J.; Neumann, B.; Rothfeld, S.; Stammler, H.-G. *Organometallics* **2004**, *23*, 6140. (b) Braun, T.; Foxon, S. P.; Perutz, R. N.; Walton, P. H. *Angew. Chem.* **1999**, *111*, 3543; *Angew Chem., Int. Ed.* **1999**, *38*, 3326. (c) Burling, S.; Elliott, I. P.; Jasim, N. A.; Lindup, R. J.; McKenna, J.; Perutz, R. N.; Archibald, S. J.; Whitwood, A. C. *Dalton Trans.* **2005**, 3686. (d) Archibald, S. J.; Braun, T.; Gaunt, J. F.; Hobson, J. E.; Perutz, R. N. *J. Chem. Soc., Dalton Trans.* **2000**, 2013. (e) Sladek, M. I.; Braun, T.; Neumann, B.; Stammler, H.-G. *J. Chem. Soc., Dalton Trans.* **2002**, 297. (f) Cronin, L.; Higgitt, C. L.; Karch, R.; Perutz, R. N. *Organometallics* **1997**, *16*, 4920. (g) Whittlesey, M. K.; Perutz, R. N.; Moore, M. H. *Chem. Commun.* **1996**, 787. (h) Braun, T.; Sladek, M. I.; Neumann, B.; Stammler, H.-G. *New. J. Chem.* **2003**, *27*, 313. (i) Vela, J.; Smith, J. M.; Yu, Y.; Ketterer, N. A.; Flaschenriem, C. J.; Lachicotte, R. J.; Holland, P. L. *J. Am. Chem. Soc.* **2005**, *127*, 7857. (j) Lindup, R. J.; Marder, T. B.; Perutz, R. N.; Whitwood, A. C. *Chem. Commun.* **2007**, 3664.

(6) (a) McGrady, J. E.; Perutz, R. N.; Reinhold, M. *J. Am. Chem. Soc.* **2004**, *126*, 5268. (b) Bosque, R.; Clot, E.; Fantacci, S.; Maseras, F.; Eisenstein, O.; Perutz, R. N.; Renkema, K. B.; Caulton, K. G. *J. Am. Chem. Soc.* **1998**, *120*, 12634.

(7) (a) Hofmann, P.; Unfried, G. *Chem. Ber.* **1992**, *125*, 659. (b) Jakt, M.; Johannissen, L.; Rzepa, H. S.; Widdowson, D. A.; Wilhelm, R. *J. Chem. Soc., Perkin Trans.* **2002**, *2*, 576.

(8) Fahey, D. R.; Mahan, J. E. *J. Am. Chem. Soc.* **1977**, *99*, 522.

(9) Bach, I.; Pörschke, K.-R.; Goddard, R.; Kopiske, C.; Krüger, C.; Rufinska, A.; Seevogel, K. *Organometallics* **1996**, *15*, 4959.

(10) Braun, T.; Cronin, L.; Higgitt, C. L.; McGrady, J. E.; Perutz, R. N.; Reinhold, M. *New J. Chem.* **2001**, *25*, 19.

(11) (a) Schaub, T.; Radius, U. *Chem.—Eur. J.* **2005**, *11*, 5024. (b) Schaub, T.; Backes, M.; Radius, U. *Organometallics* **2006**, *25*, 4196. (c) Schaub, T.; Backes, M.; Radius, U. *J. Am. Chem. Soc.* **2006**, *128*, 15964. (d) Schaub, T.; Radius, U. Z. *Anorg. Allg. Chem.* **2006**, *632*, 981. (e) Schaub, T.; Döring, C.; Radius, U. *Dalton Trans.* **2007**, 1993. (f) Schaub, T.; Backes, M.; Radius, U. *Chem. Commun.* **2007**, 2037. (g) Schaub, T.; Radius, U. Z. *Anorg. Allg. Chem.* **2007**, *633*, 2168.

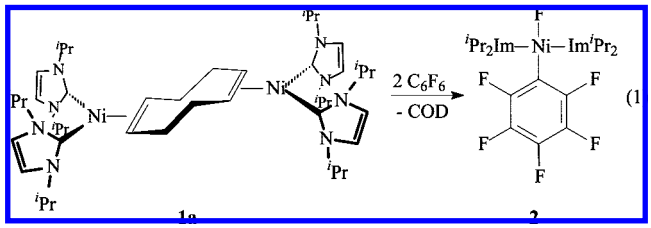

The 300 MHz proton NMR spectrum of **2** at room temperature in deuterobenzene reveals a well refined septet at 6.46 ppm for the *iso*propyl methine hydrogen atoms, a singlet at 6.31 ppm for the hydrogen atoms of the carbene backbone and two broad resonances at 1.38 ppm and 1.10 ppm for the *iso*propyl methyl hydrogen atoms. Proton NMR spectra of **2** recorded at different temperatures are given in Figure 1.

At the high temperature limit at 363 K in d_8-toluene we observed a well resolved doublet for the ^{i}Pr methyl hydrogen atoms at 1.29 ppm with a coupling constant of 6.6 Hz, a septet at 6.46 ppm for the ^{i}Pr methine hydrogen atoms and a singlet at 6.37 ppm for the hydrogen atoms of the carbene backbone. This signal pattern is in accordance with a *trans* configuration of the carbene ligands of the diamagnetic, square planar complex **2**. Whereas the singlet of the backbone hydrogen atoms and the septet for the ^{i}Pr methine hydrogen atoms remain unaltered upon cooling, the doublet at 1.29 ppm broadens significantly at 323 and 313 K, and finally splits into two resonances (Figure 1). At 273 K two well-resolved doublets appear at 1.06 and 1.36 ppm for the carbene methyl groups with coupling constants of 6.6 Hz. We attribute this dynamic behavior to a hindered rotation of the carbene ligand about the Ni−$C_{carbene}$ axis, that is, the passing of the bulky ^{i}Pr groups through the coordination plane is restricted. If this process is slow on the NMR time scale, the methyl groups at each ^{i}Pr substituent of the carbene ligand are diastereotopic and become prochiral. The estimated free enthalpy is 62.8 kJ/mol at the coalescence temperature 313 K.[12] Note that the carbene ligands have apparently enough flexibility to give only two sets of signals for the methyl protons and one set for the methine hydrogens.

Crystals of **2** suitable for X-ray diffraction have been obtained from solutions in wet toluene. Despite several attempts, we could not crystallize **2** in rigorously dried solvent, but in the presence of traces of water complex **2** crystallizes readily, stabilized with one water molecule in the elemental cell. As shown in Figure 2, complex **2** adopts a square planar geometry with a *trans* alignment of the carbene ligands in the solid state confirming the proposed structure. The additional water molecule in the cell is bound to **2** via a hydrogen bond to the fluoro ligand (distance F(1)−H(1b), 1.712 Å; distance F(1)-O, 2.609 Å; angle Ni−F(1)−O, 115°). Comparable stabilization effects of hydrogen bonds to group 10 metal fluoros have been observed before.[5a–c,13] The general principles of hydrogen bonding to halide ligands are summarized in Brammer's review.[13a] The bond length Ni−F of 1.8908(12) Å in **2** is comparable to the distances found in other nickel phosphine complexes, but also to the separations found in *trans*-[Ni(^{i}Pr$_2$Im)$_2$(F)(4-(CF$_3$)C$_6$F$_4$)] **3**[11c] and *trans*-[Ni(^{i}Pr$_2$Im)$_2$(F)(4-(SiMe$_3$)C$_6$F$_5$)] **5** (*vide infra*) (benzene ligands are numbered with the nickel in the position 1; naphthalene units are numbered according to the IUPAC numbering of the parent compound with nickel in the position

(12) Fribolin, H. *Ein- und Zweidimensionale NMR-Spektroskopie* (One- and Two-Dimensional NMR Spectroscopy); Wiley-VCH: Weinheim, Germany, 1999; p 307.

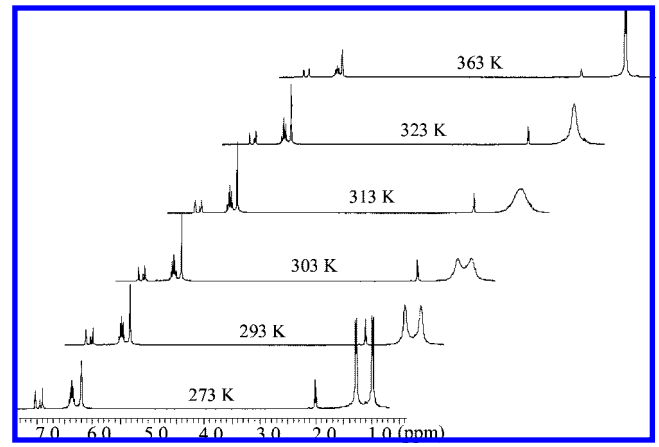

Figure 1. Proton NMR spectra of **2** (300 MHz) in d_8-toluene in the region between 0.00 ppm and 7.50 ppm recorded at different temperatures.

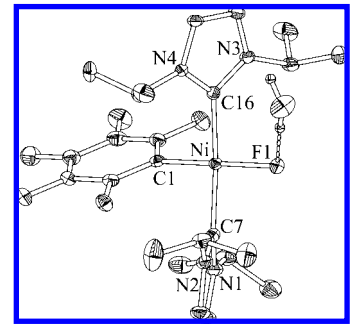

Figure 2. ORTEP diagram of the molecular structure of *trans*-[Ni(^{i}Pr$_2$Im)$_2$(F)(C$_6$F$_5$)]·H$_2$O, **2·H$_2$O**, in the solid state (ellipsoids set at 40% probability level). Hydrogen atoms bound at O(1) were located in the difference Fourier map and refined isotropically. All hydrogen atoms at calculated positions have been omitted for clarity. Selected bond lengths (Å) and angles (deg): Ni−F(1), 1.891(1); Ni−C(1), 1.907(2); Ni−C(7), 1.924(2); Ni−C(16), 1.933(2); O−H(1A), 0.83(4); O−H(1B), 0.90(4); F(1)−Ni−C(1), 175.45(8); F(1)−Ni−C(7), 89.89(7); C(1)−Ni−C(7), 90.21(8); F(1)−Ni−C(16), 88.62(7); H(1A)−O−H(1B) 109(3).

1 or 2). The fluoro and pentafluorophenyl ligands are located in a mutual *trans* position, the angle F(1)−Ni−C(1) is 175.45(8)°, and the aryl plane is twisted by 66.7° with respect to the plane defined by the atoms C(1), F(1), C(7), and C(16). The planes defined by the carbene atoms N(1), C(7), N(2), and N(4), C(16), N(3) intersect each other by an angle of 46.4(2)°. The Ni−C(1) distance to the *ipso* carbon atom of the pentafluoroarene ring of 1.9072(19) Å is shorter than the Ni−C distances to the carbene ligand (1.924(2) and 1.9329(19) Å), but comparable to Ni−C distances observed for other nickel (II) aryl complexes such as in *trans*-[Ni(PMe$_3$)$_2$(Ph)(Br)] (1.891 Å) and *trans*-[Ni(PPh$_3$)$_2$(Ph)(Cl)] (1.887 Å).[14]

Since **1a** activates the C−F bond of hexafluorobenzene very efficiently, we were led to further investigate C−F activation

(13) (a) See for example: Brammer, L. *Dalton Trans.* **2003**, 3145. (b) Jasim, N. A.; Perutz, R. N. *J. Am. Chem. Soc.* **2000**, *122*, 8685. (c) Grushin, V. V.; Marshall, W. *J. Angew. Chem.* **2002**, *114*, 4656; *Angew. Chem., Int. Ed.* **2002**, *41*, 4476. (d) Noveski, D.; Braun, T.; Krückemeier, S. *J. Fluorine Chem.* **2003**, *125*, 959. (e) Pilon, M. C.; Grushin, V. V. *Organometallics* **1998**, *17*, 1774. (f) Roe, D. C.; Marshall, W. J.; Davidson, F.; Soper, P. D.; Grushin, V. V. *Organometallics* **2000**, *19*, 4575. (g) Fraser, S. L.; Antipin, M. Y.; Khroustalyov, V. N.; Grushin, V. V. *J. Am. Chem. Soc.* **1997**, *119*, 4769. (h) Gil-Rubio, J.; Weberndörfer, B.; Werner, H. *J. Chem. Soc., Dalton Trans.* **1999**, 1437. (i) Vincente, J.; Gil-Rubio, J.; Bautista, D.; Sironi, A.; Masciocchi, N. *Inorg. Chem.* **2004**, *43*, 5665.

Scheme 1. Reaction of $[Ni_2(^iPr_2Im)_4(COD)]$ (**1a**) with Different Fluorinated Aromatic Compounds[a]

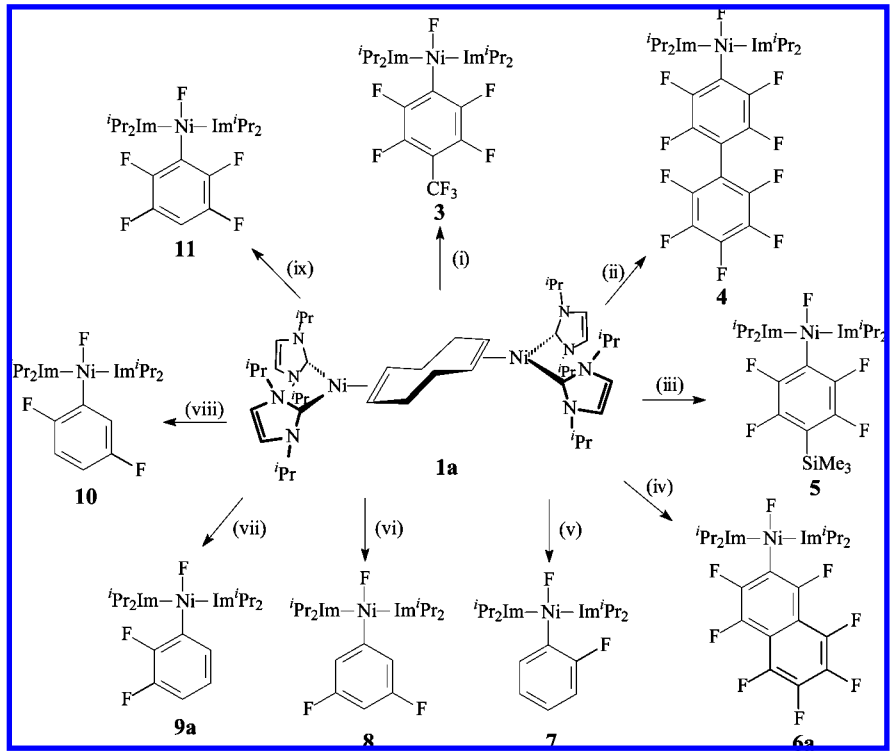

[a] Reagents, conditions, and yields of isolated products: (i) C_7F_8, THF, room temp, 75%; (ii) $C_{12}F_{10}$, THF, room temp, 54%; (iii) $C_6F_5-SiMe_3$, THF, room temp, 61%; (iv) $C_{10}F_8$, THF, room temp, 60%, (v) 1,2-$C_6F_2H_4$, THF, room temp, 73%; (vi) 1,3,5-$C_6F_3H_3$, THF, room temp, 58%; (vii) 1,2,3-$C_6F_3H_3$, THF, room temp, 65%; (viii) 1,2,4-$C_6F_3H_3$, THF, room temp, 55%; (ix) C_6F_5H, THF, −78 °C, 60%.

reactions of fluorinated arenes with complex **1a** in more detail. One focus of the studies has been the regio- and chemoselectivity of these reactions. The results are summarized in Scheme 1.

Reactions of **1a** with different fluorinated aromatic compounds in THF, benzene, or toluene occur with a high chemo- and regioselectivity. On using polyfluorinated aromatics of the type C_6F_5X such as octafluorotoluene (X = CF_3), trimethyl(pentafluorophenyl)silane (X = $SiMe_3$), or decafluorobiphenyl (X = C_6F_5) the C−F activation takes regioselectively place at the C−F bond in the *para* position to the X group to afford the complexes *trans*-$[Ni(^iPr_2Im)_2(F)(4\text{-}(CF_3)C_6F_4)]$ **3**, *trans*-$[Ni(^iPr_2Im)_2(F)(4\text{-}(C_6F_5)C_6F_4)]$ **4**, and *trans*-$[Ni(^iPr_2Im)_2(F)(4\text{-}(SiMe_3)C_6F_4)]$ **5**. Complex $[Ni_2(^iPr_2Im)_4(COD)]$ **1a** also activates C−F bonds of fused arenes, as exemplified by the formation of *trans*-$[Ni(^iPr_2Im)_2(F)(1,3,4,5,6,7,8\text{-}C_{10}F_7)]$ **6a** from the reaction of **1a** with stoichiometric amounts of octafluoronaphthalene. This reaction is quantitative when performed in an NMR tube raising the temperature slowly from −100 °C to room temperature and yields, in contrast to the reaction of **1b** with octafluoronaphthalene (*vide infra*), exclusively to an insertion into the C−F bond in the 2-position of the octafluoronaphthalene. In the ^{19}F NMR seven signals were detected in the range between −95.1 and −160.2 ppm which can be assigned to the organyl ligand. One signal at −372.5 ppm is characteristic for the fluoro ligand.

On using partially fluorinated aromatic substrates such as 1,2-difluorobenzene, 1,3,5-trifluorobenzene, 1,2,3-trifluorobenzene, and 1,2,4-trifluorobenzene, the C−F activation products *trans*-$[Ni(^iPr_2Im)_2(F)(2\text{-}C_6FH_4)]$ **7**, *trans*-$[Ni(^iPr_2Im)_2(F)(3,5\text{-}C_6F_2H_3)]$ **8**, *trans*-$[Ni(^iPr_2Im)_2(F)(2,3\text{-}C_6F_2H_3)]$ **9a** and *trans*-$[Ni(^iPr_2Im)_2(F)(2,6\text{-}C_6F_2H_3)]$ **9b**, *trans*-$[Ni(^iPr_2Im)_2(F)(2,5\text{-}C_6F_2H_3)]$ **10**, and *trans*-$[Ni(^iPr_2Im)_2(F)(2,3,5,6\text{-}F_4C_6H)]$ **11** have been isolated in good to moderate yields. On the NMR scale these reactions are quantitative according to ^1H and ^{19}F NMR spectroscopy. In all cases the activation of the C−F-bond prevails over C−H activation. The reaction of **1a** with 1,2,3-trifluorobenzene at −78 °C leads to a mixture of the isomers *trans*-$[Ni(^iPr_2Im)_2(F)(2,3\text{-}C_6F_2H_3)]$ **9a** and *trans*-$[Ni(^iPr_2Im)_2(F)(2,6\text{-}C_6F_2H_3)]$ **9b**. The activation product of the statistically more favored C−F bonds in the 1-position is the major isomer (approximately 85% judged by ^{19}F NMR spectroscopy). Minor amounts (approximately 15%) of the second isomer arise from an activation of the 2-position in the substrate, and we speculate that the formation of *trans*-$[Ni(^iPr_2Im)_2(F)(2,3\text{-}C_6F_2H_3)]$ **9a** is preferred for kinetic reasons, because C−F bonds in the ortho position to the metal have been associated with the strongest metal−carbon bond to the fluorinated ring.[15] Note also that usually cleavage of the strongest bond of the substrate will lead to the strongest bonds of the substrate's fragments to the metal.[15,16] If the reaction of **1a** with 1,2,3-trifluorobenzene is performed at room temperature, we obtained a comparable product distribution as at −78 °C. A

(14) (a) Klein, H.-F.; Bickelhaupt, A.; Lemke, M.; Sun, H.; Brand, A.; Jung, T.; Röhr, C.; Flörke, U.; Haupt, H.-J. *Organometallics* **1997**, *16*, 668. (b) Zeller, A.; Herdtweck, E.; Strassner, T. *Eur. J. Inorg. Chem.* **2003**, 1802.

(15) (a) Clot, E.; Oelckers, B.; Klahn, A. H.; Eisenstein, O.; Perutz, R. N. *Dalton Trans.* **2003**, 4065. (b) Clot, E.; Besora, B. M.; Maseras, F.; Megret, C.; Eisenstein, O.; Oelckers, B.; Perutz, R. N. *Chem. Commun.* **2003**, 490.

(16) (a) Nolan, S. P.; Hoff, C. D.; Stoutland, P. O.; Newman, L. J.; Buchanan, J. M.; Bergman, R. G.; Yang, G. K.; Peters, K. S. *J. Am. Chem. Soc.* **1987**, *109*, 3143. (b) Stoutland, P. O.; Bergman, R. G.; Nolan, S. P.; Hoff, C. D. *Polyhedron* **1988**, *7*, 1429. (c) Bryndza, H. E.; Fong, L. K.; Paciello, R. A.; Tam, W.; Bercaw, J. E. *J. Am. Chem. Soc.* **1987**, *109*, 1444.

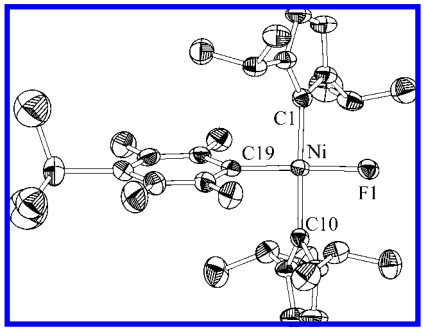

Figure 3. ORTEP diagram of the molecular structure of *trans*-[Ni(^{i}Pr$_2$Im)$_2$-(F)(4-(SiMe$_3$)C$_6$F$_4$)] (**5**) in the solid state (ellipsoids set at 40% probability level). Hydrogen atoms have been omitted for clarity. Selected bond lengths (Å) and angles (deg): Ni−F(1), 1.856(3); Ni−C(1), 1.911(6); Ni−C(10), 1.905(6); Ni−C(19), 1.873(6); F(1)−Ni−C(1), 89.4(2); F(1)−Ni−C(10), 89.0(2); F(1)−Ni−C(19), 177.7(2); C(1)−Ni−C(10), 175.0(2); C(1)−Ni−C(19), 92.1(3); C(10)−Ni−C(19), 89.7(2).

possible C−H activation product is in this case not feasible presumably because of the weakness of the Ni−H bond in comparison to the Ni−F bond.[6a]

The complexes **2**−**11** have been characterized by proton and fluorine NMR spectroscopy and IR spectroscopy as well as mass spectrometry and/or elemental analysis. As described for the pentafluoroarene complex **2**, the proton NMR spectra of these compounds show at room temperature two broad resonances for the carbene *iso*propyl methyl hydrogen atoms in the region between 1.00 and 1.45 ppm, a septet for the *iso*propyl methine hydrogen atoms at approximately 6.50 ppm and a singlet at approximately 6.20 ppm for the carbene olefinic protons. The fluoro ligands give rise to signals in the region between −350 to −375 ppm in the ^{19}F NMR spectra.

Crystals suitable for X-ray diffraction of the complex *trans*-[Ni(^{i}Pr$_2$Im)$_2$(F)(4-(SiMe$_3$)C$_6$F$_4$)] **5** have been obtained from a saturated diethylether/hexane (3:1) solution at −40 °C. The molecular structure of **5** (Figure 3) reveals a square planar coordinated nickel atom, in which both carbene ligands are in a trans position to each other. Similarly to the values found in the molecular structure of **2**, the Ni−C$_{carbene}$ distances fall in the narrow region between 1.90 and 1.92 Å. The Ni−F distance of 1.856(3) Å is shorter than the Ni−F distance found in **2** (1.891(1) Å) due to the lack of fluorine−hydrogen bonding. In accordance to the spectroscopic data, the molecular structure clearly reveals that the C−F activation took place in the *para* position to the SiMe$_3$ group.

One recent focus of oxidative addition reactions of carbon−fluorine bonds at nickel has been on the C−F activation of fluorinated heterocycles.[1f,3,5] The reactions have been stimulated by an interesting chemo- and regioselectivity. For instance, treatment of [Ni(COD)$_2$] with pentafluoropyridine in the presence of PEt$_3$ has been shown to give *trans*-[Ni(PEt$_3$)$_2$(F)(2-C$_5$NF$_4$)] with a preference for a cleavage at the 2-position of pentafluoropyridine. In contrast, carbon−fluorine bond activation reactions of pentafluoropyridine at Pt, Pd, and Rh led to an activation at the 4-position.[5a,2i,17] The unusual regioselectivity at nickel has been attributed to an oxidative addition via a concerted reaction pathway. Because of the high reactivity and nucleophilicity of the {Ni(^{i}Pr$_2$Im)$_2$} moiety, we were also

Scheme 2. Activation of Pentafluoropyridine with [Ni(^{i}Pr$_2$Im)$_2$(η^2-C$_2$H$_4$)] **1b**

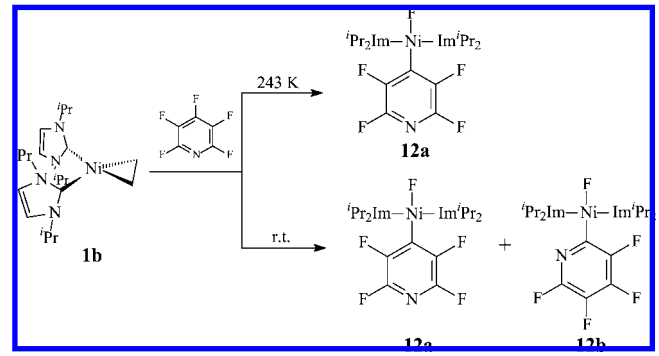

interested in the selectivity of reactions of [Ni$_2$(^{i}Pr$_2$Im)$_4$(COD)] **1a** and [Ni(^{i}Pr$_2$Im)$_2$(η^2-C$_2$H$_4$)] **1b** with pentafluoropyridine.

Treatment of a solution of **1a** or of **1b** with pentafluoropyridine at low temperatures (195 K in the case of **1a** and 243 K in the case of **1b** leads to the generation of *trans*-[Ni(^{i}Pr$_2$Im)$_2$(F)(4-C$_5$NF$_4$)] **12a** as the sole product of the reaction (Scheme 2) (2-, 3-, and 4- indicate the relative position of the nickel atom to the ring nitrogen atom in pentafluoropyridine complexes (*ortho*, *meta*, *para* position)). In contrast, the reaction of **1b** with pentafluoropyridine at room temperature leads to the generation of *trans*-[Ni(^{i}Pr$_2$Im)$_2$(F)(4-C$_5$NF$_4$)] **12a** and *trans*-[Ni(^{i}Pr$_2$Im)$_2$(F)(2-C$_5$NF$_4$)] **12b**. A ^{19}F NMR spectrum of the reaction mixture indicates that **12a** and **12b** are formed in a ratio of approximately 1:2.

The two tetrafluoropyridyl complexes can be distinguished by their ^{19}F NMR data. Complex **12b** exhibits four resonances for the four inequivalent fluorine nuclei at −86.8, −133.8, −152.3, and −174.5 ppm. These data are consistent with an assignment of **12b** as a 2-nickel derivative of pentafluoropyridine and are not compatible with an isomer bearing the nickel in the 3-position.[2h,5h] The spectrum of the 4-nickel derivative **12a** shows only two signals at −100.6 and −120.7 ppm. The fluoro ligand at each isomer is characterized by an additional signal at −354.7 (**12b**) and −369.3 (**12a**) ppm.

Intermediates of C−F Bond Activation Reactions. In earlier work the oxidative addition of fluorinated aromatics and heteroaromatics such as hexafluorobenzene, pentafluoropyridine, and 2,4,6-trifluoropyrimidine at a nickel(0)bisphosphine fragment has been studied.[1,5,6] At {Ni(PEt$_3$)$_2$} it turned out that the activation of hexafluorobenzene and related polyfluorinated substrates are much slower compared to the activation of pentafluoropyridine and 2,4,6-trifluoropyrimidine.[5] To gain some information on the mechanism of the rapid C−F activation reactions at {Ni(^{i}Pr$_2$Im)$_2$}, we were interested in the detection of intermediates along with kinetic studies. Although the work described above has pointed out that the COD complex [Ni$_2$(^{i}Pr$_2$Im)$_4$(COD)] **1a** is slightly more active for C−F activation than the ethylene complex [Ni(^{i}Pr$_2$Im)$_2$(η^2-C$_2$H$_4$)] **1b**, we performed these studies using **1b** as starting compound, because of the limited solubility of **1a** in toluene and THF at low temperatures. In addition, the COD, which is liberated during a reaction, might hamper the reaction kinetics.

Treatment of [Ni(^{i}Pr$_2$Im)$_2$(η^2-C$_2$H$_4$)] **1b** with hexafluorobenzene at 193 K leads to the formation of a new complex (**13**), which exhibits a coordinated hexafluorobenzene at the metal center (Scheme 3). The ^{19}F NMR spectrum at 193 K of the reaction solution shows one broad signal at −169.2 ppm consistent with a fluxional structure. Upon warming the solution

(17) (a) Braun, T.; Rothfeld, S.; Schorlemer, V.; Stammler, A.; Stammler, H.-G. *Inorg. Chem. Commun.* **2003**, *6*, 752. (b) Braun, T.; Steffen, A.; Schorlemer, V.; Neumann, B.; Stammler, H.-G. *Dalton Trans.* **2005**, 3331.

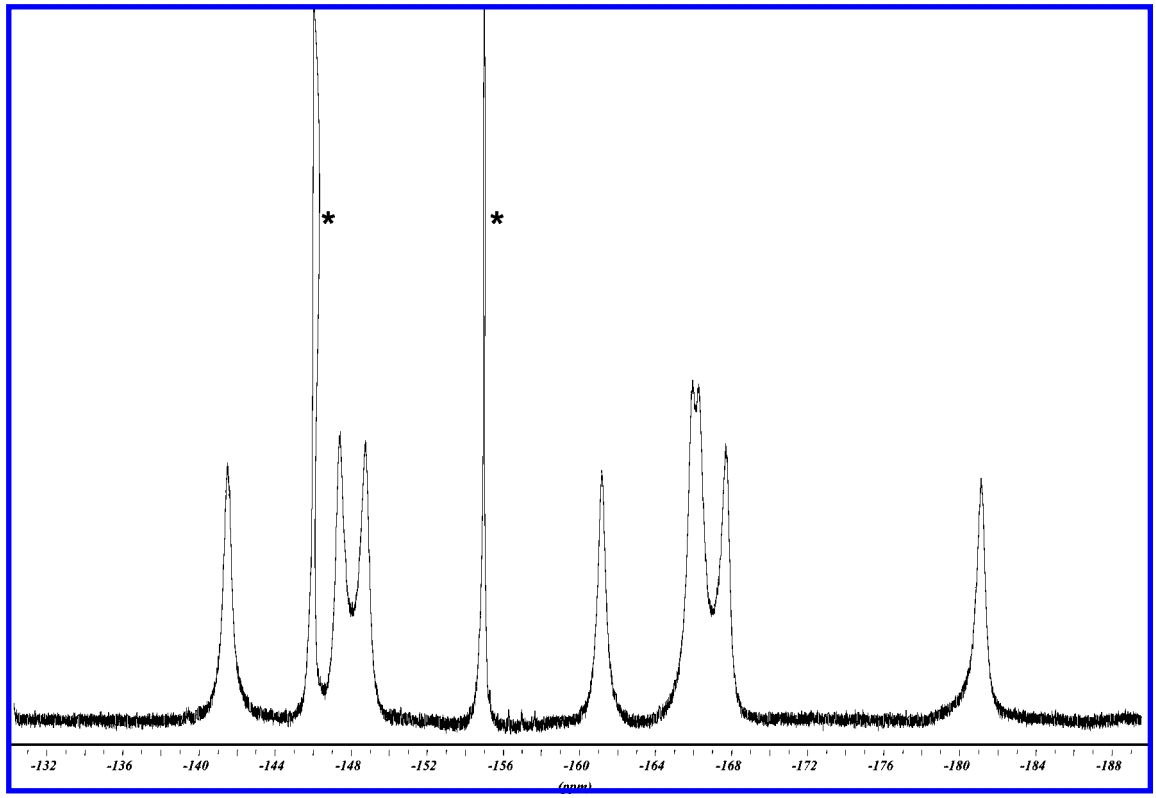

Figure 4. ^{19}F NMR spectrum of [Ni(^{i}Pr$_2$Im)$_2$(η^2-C$_{10}$F$_8$)] **14** (564.6 MHz) at 243 K in d_8-toluene; the asterisk (∗) indicates free octafluoronaphthalene.

Scheme 3. Reaction of [Ni(^{i}Pr$_2$Im)$_2$(η^2-C$_2$H$_4$)] **1b** with Perfluorobenzene and Octafluoronaphthalene *via* Intermediates with η^2-Coordinated Perfluoroarene Ligand

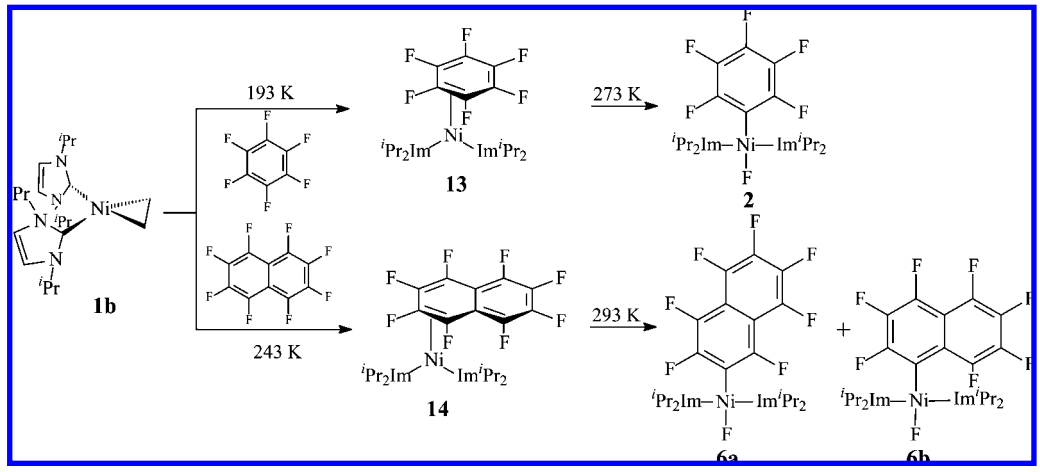

the signal sharpens. We assign complex **13** as [Ni(^{i}Pr$_2$Im)$_2$(η^2-C$_6$F$_6$)], although binuclear complexes or other coordination modes can not be excluded entirely.[1,7a,18] A comparable compound [Ni(^{t}Bu$_2$PC$_2$H$_4$P^{t}Bu$_2$)(η^2-C$_6$F$_6$)] has been isolated by Pörschke and co-workers ($\delta_F = -166.9$ ppm).[9] Complex **13** is only stable in the presence of free hexafluorobenzene and converts at 273 K into the C−F activation product [Ni(^{i}Pr$_2$Im)$_2$(F)(C$_6$F$_5$)] **2**.

A reaction of [Ni(^{i}Pr$_2$Im)$_2$(η^2-C$_2$H$_4$)] **1b** with octafluoronaphthalene at 243 K affords the complex [Ni(^{i}Pr$_2$Im)$_2$(η^2-C$_{10}$F$_8$)] **14**, which exhibits a coordinated naphthalene molecule in an η^2-mode (see Scheme 3). The ^{19}F NMR spectrum of **14** at 243 K (564.6 MHz) displays eight broad signals at −141.5, −147.4, −148.8, −161.2, −166.0, −166.3, −167.7, and −181.1 ppm for the inequivalent fluorine nuclei (Figure 4). Spectra below that temperature show a comparable pattern. Note that for [Ni(PEt$_3$)$_2$(η^2-C$_{10}$F$_8$)] only four resonances could be observed at low temperature.[10]

Figure 5 displays ^{19}F NMR spectra of **14** (564.6 MHz) at different temperatures. The spectra indicate a fluxional behavior. Coalescence for two pairs of signals at −147.4/−148.8 and −166.3/−167.7 ppm can be observed at approximately 253 K. Coalescence between the resonances at −161.2 and −166.0 ppm

(18) (a) Higgitt, C. L.; Klahn, A. H.; Moore, M. H.; Oelckers, B.; Partridge, M. G.; Perutz, R. N. *J. Chem. Soc., Dalton Trans.* **1997**, 1269. (b) Martin, A.; Orpen, A. G.; Seeley, A. J.; Timms, P. L. *J. Chem. Soc., Dalton Trans.* **1994**, 2251. (c) Bell, T. W.; Helliwell, M.; Partridge, M. G.; Perutz, R. N. *Organometallics* **1992**, *11*, 1911. (d) McGlinchey, M. J.; Tan, T. S. *J. Am. Chem. Soc.* **1976**, *98*, 2271. (e) Barker, J. J.; Orpen, A. G.; Seeley, A. J.; Timms, P. L. *J. Chem. Soc., Dalton Trans.* **1993**, 3097.

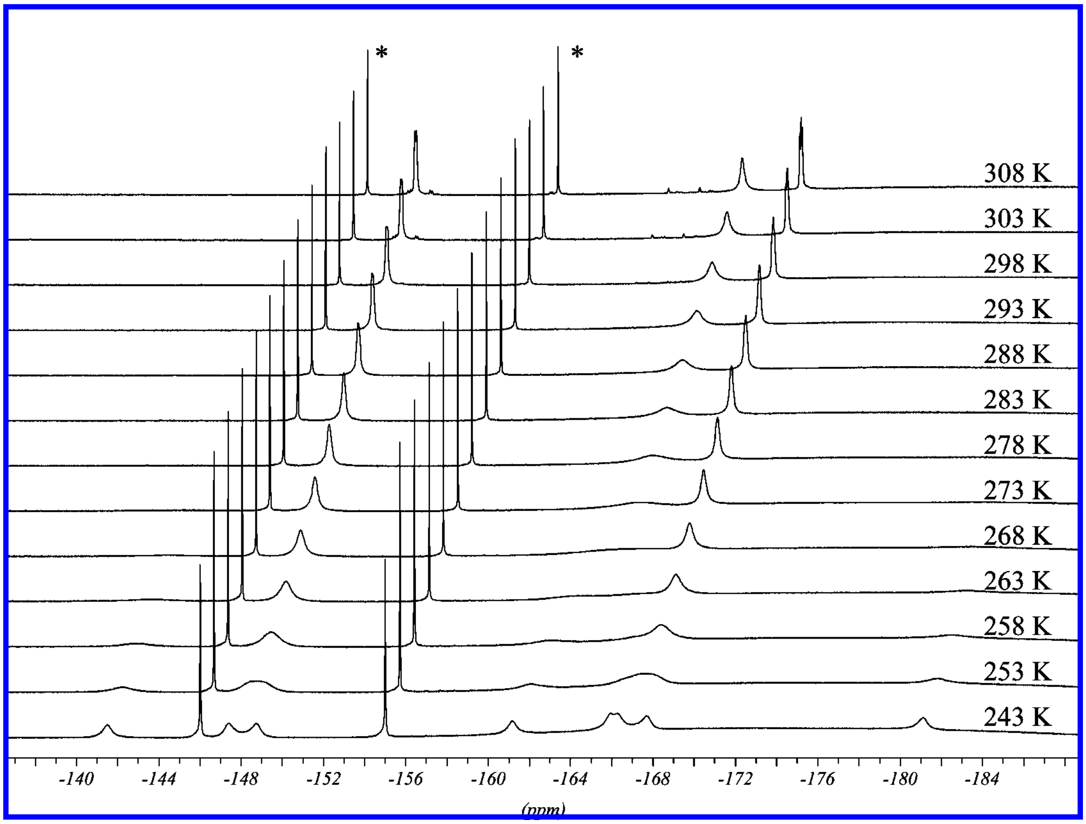

Figure 5. ^{19}F NMR spectra of $[Ni(^iPr_2Im)_2(\eta^2\text{-}C_{10}F_8)]$ **14** (564.6 MHz) at different temperatures in d_8-toluene; the asterisk (∗) indicates free octafluoronaphthalene.

was found at 268 K. The spectrum now reveals three signals at −148, −164, and −167 ppm with a ratio of 1:1:1 at 298 K. The resonances do not broaden at the same rate, and the estimated free energy at each coalescence temperature for each pair of fluorines has been estimated to be $\Delta G^{\ddagger} = 46$ kJ/mol.[12] We were not able to detect the coalescence between the signals at −141.5 and −181.1 ppm at 564.6 MHz. One has to expect an extremely broad signal, because of the huge difference in the chemical shift of the signals ($\Delta\nu = 22358$ Hz). However, a spectrum at 282.4 MHz which has been acquired rapidly at 323 K revealed an additional broad signal at –161 ppm, which appears to be due to coalescence of the resonances at −141.5 and −181.1 ppm. An EXSY/NOESY NMR spectrum at 223 K with a mixing time of 1 s (564.6 MHz) exhibits cross-peaks with a positive sign with respect to the diagonal peaks. The spectrum reveals exchange between the same four pairs of nuclei as suggested above including exchange between the fluorines which show signals at −141.5 and −181.1 ppm.

The variable temperature studies are compatible with a fluxional η^2-$C_{10}F_8$ structure. The dynamic behavior can be explained by a suprafacial 1,3-shift of the nickelbiscarbene moiety, that is, the coordination mode of the naphthalene changes from 1,2-η^2 to 3,4-η^2 (Scheme 4). There is no migration of the nickel to the second aromatic ring of the naphthalene. This leads for the eight resonances for the eight fluorines to four sets of signals at higher temperature. Such a process might occur via an η^4-arene species or an η^3-bound transition state.[9,10,19,20] Additional broadening of the signals at any

Scheme 4. Change of the Coordination Mode of the Octafluoronaphthalene Ligand in $[Ni(^iPr_2Im)_2(\eta^2\text{-}C_{10}F_8)]$ **14** from 1,2-η^2 to 3,4-η^2

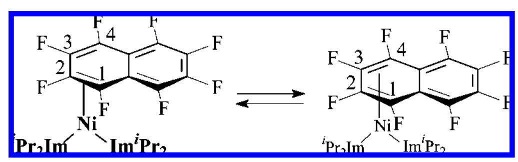

temperature is feasible due to an interconversion of two rotamers by rotation about the metal $C_{10}F_8$ interaction in an η^2-isomer.[15a] The dynamic behavior of the nickel complex $[Ni(^iPr_2PCH_2CH_2P^iPr_2)(\eta^2\text{-}C_{10}H_8)]$ has been investigated and in contrast to **14** an η^2-1,2 → η^2-3,4 as well as an η^2-1,2 → η^2-7,8 shift has been observed.[19,21] A 1,2-shift of the site of the rhenium coordination at the C_6F_6 ligand in $[Re(\eta^5\text{-}C_5H_5)(CO)_2(\eta^2\text{-}C_6F_6)]$ has been identified and the activation enthalpy has been determined to be $\Delta H^{\ddagger} = 57.6 \pm 0.5$ kJ/mol by line width analysis and exchange spectroscopy measurements.[18a] Note that rhodium η^2-naphthalene complexes also show dynamic behavior which has been explained by a pathway via a C−H activation step.[22]

A suitable crystal of complex **14** was obtained at −60 °C from a toluene/hexane solvent mixture and its structure was determined by X-ray crystallography (Figure 6). The molecular structure of **14** features an η^2-coordinated ligand compatible

(19) Benn, R.; Mynott, R.; Topalovic, I.; Scott, F. *Organometallics* **1989**, *8*, 2299.
(20) Silvestre, J.; Albright, T. A. *J. Am. Chem. Soc.* **1985**, *107*, 6829.
(21) Scott, F.; Krüger, C.; Betz, P. *J. Organomet. Chem.* **1990**, *387*, 113.
(22) (a) Chin, R. M.; Dong, L.; Duckett, S. B.; Jones, W. D. *Organometallics* **1992**, *11*, 871. (b) Chin, R. M.; Dong, L.; Duckett, S. B.; Partridge, M. G.; Jones, W. D.; Perutz, R. N. *J. Am. Chem. Soc.* **1993**, *115*, 7685. (c) Jones, W. D.; Dong, L. *J. Am. Chem. Soc.* **1989**, *111*, 8722–8723. (d) Belt, S. T.; Dong, L.; Duckett, S. B.; Jones, W. D.; Partdridge, M. G.; Perutz, R. N. *Chem. Commun.* **1991**, 266.

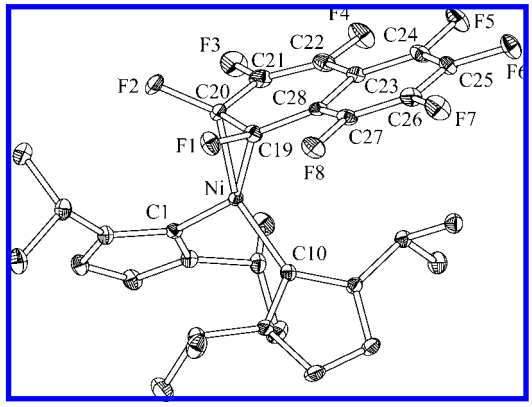

Figure 6. ORTEP diagram of the molecular structure of [Ni(^{i}Pr$_2$Im)$_2$(η^2-$C_{10}F_8$)] **14** in the solid state (ellipsoids set at 40% probability level). Hydrogen atoms have been omitted for clarity. Selected bond lengths (Å) and angles (deg): Ni−C(1), 1.939(2); Ni−C(10), 1.941(2); Ni−C(19), 1.963(2); Ni−C(20), 1.886(2); C(19)−C(20), 1.461(3); C(20)−C(21), 1.448(3); C(21)−C(22), 1.343(3); C(22)−C(23), 1.453(3); C(23)−C(24), 1.405(3); C(24)−C(25), 1.381(3); C(25)−C(26), 1.386(3); C(26)−C(27), 1.379(3); C(27)−C(28), 1.408(3); C(19)−C28), 1.460(3); F(1)−C(19), 1.411(2); F(2)−C(20), 1.413(2); F(1)−C(19)−Ni, 109.04(12); F(2)−C(20)−Ni, 125.98(13).

with the fluxional behavior via the 1,3-shift as observed in solutions of **14**. The dihedral angle between the plane defined by Ni, C(19), C(20), and the plane defined by the naphthalene ligand is 108°. The coordinated C(19)−C(20) bond of 1.461(3) Å is significantly lengthened compared to the other carbon−carbon bonds in the uncoordinated ring or compared to the corresponding bond in free octafluoronaphthalene.[23] The C(20)−C(21) bond distance is also elongated (1.448(3) Å), whereas the C(21)−C(22) separation is rather short (1.343(3) Å).[23] A comparable disruption of aromaticity has been found in [Ni(PEt$_3$)$_2$-(η^2-$C_{10}F_8$)].[10] As it has been found for the latter compound, the benzenoid ring bound to nickel is very distorted. Thus, C(19) lies 0.138 Å above the plane defined by C(19)−C(28) and 0.178 Å above the plane defined by C(21)−C(28). Consistent with that distortion, the fluorine atoms F(1) and F(2) lie out of the octafluoronaphthalene plane with F(2) 1.128 Å above the plane defined by C(19)−C(28) (Figure 6). This observation is in accordance with rather long C(19)−F(1) and C(20)−F(2) separations (1.411(2) and 1.413(2) Å) and a very short Ni−C(20) bond of 1.886(2) Å. The latter distance is within 3σ similar to the Ni−C(aryl) bond lengths of 1.9072(19), 1.876(8), and 1.860(7) Å in the C−F activation products of *trans*-[Ni(^{i}Pr$_2$Im)$_2$(F)(C_6F_5)]·H$_2$O **2·H$_2$O**, *trans*-[Ni(^{i}Pr$_2$Im)$_2$(F)(4-(CF_3)C_6F_4)] **3**, and *trans*-[Ni(^{i}Pr$_2$Im)$_2$(F)(4-($SiMe_3$)C_6F_4)] **5**. Note that the Ni−C bond lengths in [Ni(^{i}Pr$_2$PCH$_2$CH$_2$P^{i}Pr$_2$)(η^2-$C_{10}H_8$)] are 2.002(3) and 2.157(1) Å.[21]

In solution at room temperature, complex **14** converts into the products for a C−F activation of octafluoronaphthalene. In contrast to the experiments with **1a** as starting compound, we observed in this case the formation of the two isomers [Ni(^{i}Pr$_2$Im)$_2$(F)(1,3,4,5,6,7,8-$C_{10}F_7$)] **6a** and [Ni(^{i}Pr$_2$Im)$_2$(F)(2,3,4,5,6,7,8-$C_{10}F_7$)] **6b** in a ratio of 11:1. The rates for the disappearance of [Ni(^{i}Pr$_2$Im)$_2$(η^2-$C_{10}F_8$)] **14** and the formation of **6a** and **6b** were monitored by ^{19}F NMR spectroscopy in d_8-toluene at different temperatures. Because of the low solubility of **6a** and **6b**, the sum of the rates for the formation of the products did not match the rate for the disappearance of **14**.

(23) Collins, J. C.; Roscoe, K. P.; Thomas, R. L.; Batsanov, A. S.; Stimson, L. M.; Howard, J. A. K.; Marder, T. B. *New. J. Chem.* **2001**, *25*, 1410.

Table 1. Rate Constants for the Conversion of **14** into **6a/6b**

T [K]	k [10^{-5} s^{-1}]
303	0.39 ± 0.07
308	1.66 ± 0.04
313	3.68 ± 0.14
323	10.9 ± 0.29
333	49.6 ± 0.88
343	117.0 ± 1.06

However, the initial rates for the formation of **6a/6b** are similar to the rate for the loss of **14**. The rates for the disappearance of **14** are all first order and rate constants obtained are presented in Table 1. There is no dependence of the concentration of free naphthalene on the rates. A representative kinetic time course at 343 K and the corresponding plot ln{[**14**]$_t$/[**14**]$_o$} versus time are shown in Figure 7. The kinetic data fit well to the transition state theory to describe the temperature dependence of the rate constants. This is demonstrated by the Eyring plot, which is depicted in Figure 8. The activation enthalpy $\Delta H^{\ddagger}$ was determined by linear least-squares fittings to the Eyring equation. It gives an estimation of $\Delta H^{\ddagger} = 116 \pm 8$ kJ mol^{-1} ($\Delta S^{\ddagger} = 37 \pm 25$ J K^{-1} mol^{-1}).

Density Functional Theory (DFT) Calculations for the Activation of Fluorinated Aromatics. To gain more information on the energetics of the carbon−fluorine bond activation

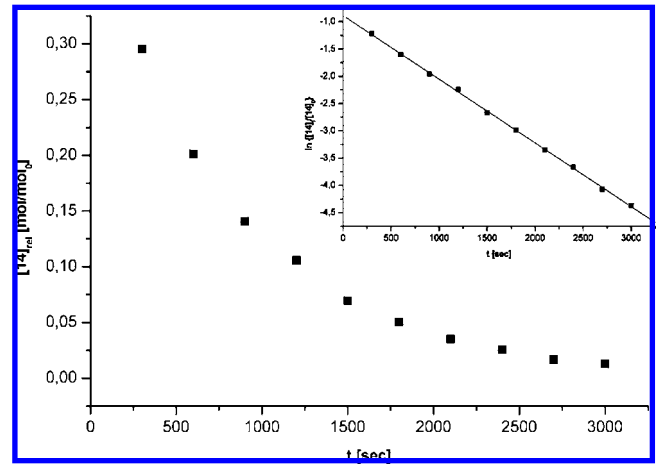

Figure 7. Kinetic time course for the loss of **14** at 343 K; plot of ln{[**14**]$_t$/[**14**]$_o$} vs time.

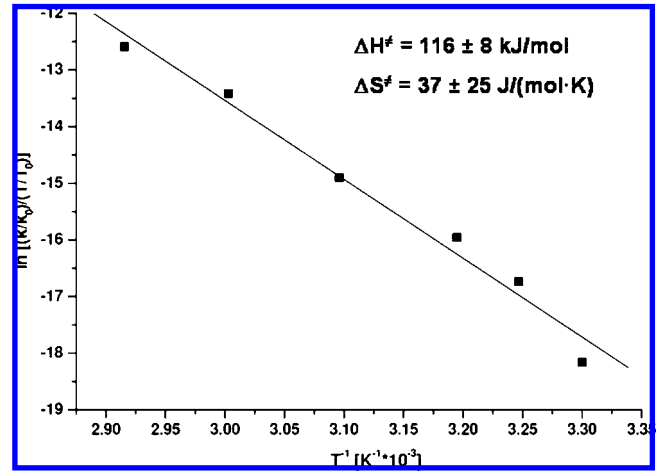

Figure 8. Eyring plot for the isomerization of **14** into **6a/6b**.

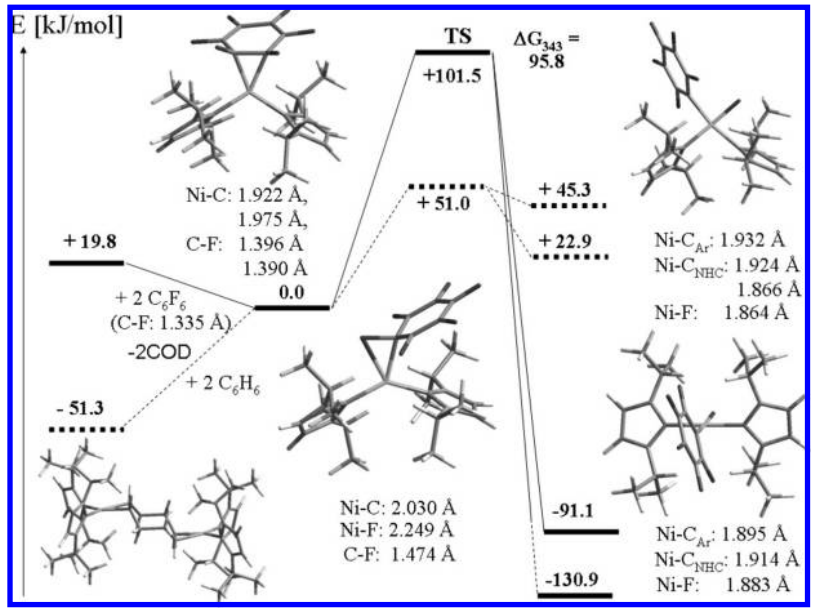

Figure 9. Calculated energetics of the C−F activation (solid lines) of C_6F_6 by $[Ni_2(^iPr_2Im)_4(COD)]$ **1a**, important geometries, and a comparison with a hypothetical C−H activation reaction of C_6H_6 (dotted lines) (energies in kJ mol^{-1}).

reactions at $\{Ni(^iPr_2Im)_2\}$, DFT calculations were performed. Because it has been shown that the steric and electronic requirements of the ligands can be crucial for the reaction pathway (i.e., for the chemo- and regioselectivity),[5b,e] the calculations have been done on the full system $\{Ni(^iPr_2Im)_2\}$. For a better comparison the major points of the energy surface of the reaction of $\{Ni(PMe_3)_2\}$ with hexafluorobenzene were also calculated, modeling an alkyl-substituted nonchelating phosphine ligand. For the latter system, we can confirm the crucial stationary points reported by McGrady and Perutz at $\{Ni(H_2PCH_2CH_2PH_2)\}$, that is, an intermediate with an η^2(C,C)-coordinated hexafluorobenzene ligand as a minimum, a transition state featuring an η^2(C,F) σ-complex and the products *cis*- and *trans*-$[Ni(PMe_3)_2(F)(C_6F_5)]$. With respect to the η^2(C,C) coordinated intermediate $[Ni(PMe_3)_2(\eta^2\text{-}\{C,C\}\text{-}C_6F_6)]$, we find that the transition state is 111.4 kJ/mol higher, the products 73.4 kJ/mol (cis), and 125.3 kJ/mol (trans) lower in energy, respectively.

Results of DFT calculations on the reaction of $[Ni_2(^iPr_2Im)_4(COD)]$ **1a** with C_6F_6 are summarized in Figure 9. The first step of the reaction should be the transfer of the $\{Ni(^iPr_2Im)_2\}$ complex fragments from **1a** to C_6F_6 to yield the η^2(C,C)-bonded reaction intermediate. This transfer is exothermic (19.8 kJ/mol per complex fragment) according to our calculations and in good agreement with the experiments described above, which have shown that the complex $[Ni(^iPr_2Im)_2(\eta^2\text{-}C_6F_6)]$ is readily available from the reaction of **1a** or **1b** with C_6F_6.

The geometric data of the optimized structure of $[Ni(^iPr_2Im)_2(\eta^2\text{-}C_6F_6)]$ (see Figure 9) are compatible with the distances and angles which have been found for the molecular structure of **14**. The nickel atom is asymmetrically coordinated to the C_6F_6 ring; we calculate Ni−C distances of 1.9219 and 1.9748 Å at the level of theory employed. The plane defined by Ni and the carbene carbon atoms and the plane defined by Ni and the hexafluorobenzene carbon atoms attached to the nickel atom intersect each other by 12.15°; the best plane through the C_6F_6 ligand and the plane defined by Ni and the carbene carbon atoms form an angle of 111.6°. The six-membered ring of the C_6F_6 ligand is planar; the carbon atoms deviate from the best plane by less than 0.09 Å. The fluorine substituents at the coordinated carbon atoms are strongly bent (38.9° and 26.1°, respectively) out of this plane (0.9468 and 0.5014 Å from the plane), away from the Ni atom. All other fluorine substituents on adjacent C atoms are only slightly bent away from the nickel atom (6.4° as a maximum). The coordinated C−C bond is substantially lengthened (1.474 vs 1.461 Å in **14** vs 1.39 Å in C_6F_6). The C−C bonds of the C_6F_6 ligand display a strong alternation of bond lengths (1.474 vs 1.445/1.449 vs 1.380/1.379 vs 1.437 Å going from the coordinated CC unit through the ring), consistent with charge localization upon coordination of the $\{Ni(^iPr_2Im)_2\}$ entity. Note that the C−F bonds at the coordinated carbon centers are already elongated relative to the uncoordinated ligand (1.396 and 1.390 vs 1.335 Å).

The calculated structure *trans*-$[Ni(^iPr_2Im)_2(F)(C_6F_5)]$ of the C−F activation (see Figure 9) product is also in excellent agreement with the molecular structure determined for *trans*-$[Ni(^iPr_2Im)_2(F)(C_6F_5)]$ **2**, showing a square-planar coordination of the nickel atom and bond lengths as observed for **2** (Ni−F, 1.883 vs 1.891(1) Å in **2**; Ni−C_{Ar}, 1.895 vs 1.907(2) Å in **2**; Ni−$C_{carbene}$, 1.914 vs 1.923(2) Å on average in **2**). The planes defined by the carbene atoms (see Figure 2: N(1), C(7), N(2), and N(4), C(16), N(3)) intersect each other by an angle of 35.9° (exptl, 46.4°) for the calculated structure and the aryl plane is twisted by 72.2° (exptl, 66.7°) with respect to the plane defined through the coordination plane (C(1), F(1), C(7), and C(16), see Figure 2). For the *cis* isomer, the lengths of the Ni−$C_{carbene}$ bonds are significantly different, the one in the *trans* position to the C_6F_5 group being 0.06 Å longer as a result of the stronger *trans* influence of the pentafluorophenyl ligand. The calculated total energies indicate that the oxidative addition product is 91.1 kJ/mol (*cis* product) or 130.9 kJ/mol (*trans* product) more stable than the η^2(C,C) coordinated intermediate, which in turn is 19.8 kJ/mol more stable than the reactants. We never observed a *cis* configured product during our investigations and therefore assume that *cis*−*trans* isomerization is rapid.

The transition state leading to a cleavage of the C−F bond has been located 101.5 kJ/mol above the η^2(C,C) intermediate.

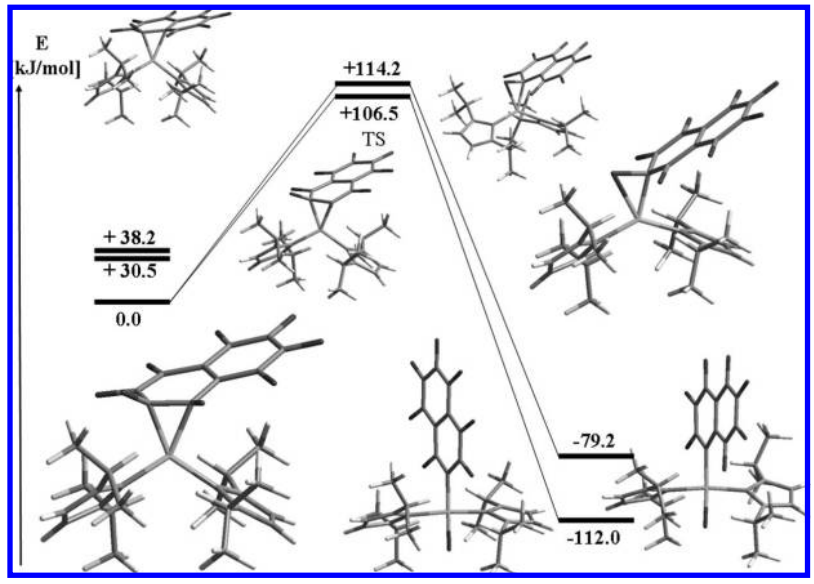

Figure 10. Calculated energetics of the C−F activation of $C_{10}F_8$ by $[Ni_2(^iPr_2Im)_4(COD)]$ **1a** (energies in kJ mol^{-1}).

This barrier is approximately 10 kJ/mol lower in energy than the corresponding barrier for the PMe_3 stabilized system (111.4 kJ/mol). The data are in accordance with the activation parameter deduced from NMR spectroscopy for the conversion of the naphthalene complex $[Ni(^iPr_2Im)_2(\eta^2\text{-}C_{10}F_8)]$ **14** to the oxidative addition products *trans*-$[Ni(^iPr_2Im)_2(F)(1,3,4,5,6,7,8\text{-}C_{10}F_7)]$ **6a** and *trans*-$[Ni(^iPr_2Im)_2(F)(2,3,4,5,6,7,8\text{-}C_{10}F_7)]$ **6b** (116 ± 8 kJ/mol). The transition state features a η^2(C,F) σ-coordinated ligand in which the C−F bond length of 1.474 Å is significantly elongated compared to the C−F distance in C_6F_6 (1.335 Å), but only 0.09 Å longer than that calculated for the η^2(C,C) coordinated intermediate. The arene ring is oriented such that the sp^2 hybrid orbital on the *ipso* carbon is involved into bonding to the fluorine and to the nickel atom. The C−F bond lies thus almost exactly in the $C_{carbene}$−Ni−$C_{carbene}$ plane (the angle between planes defined by the atoms $C_{carbene}$, Ni, $C_{carbene}$, and Ni, C−F is 10.95°) to maximize the overlap between the C−F σ^* orbital and the HOMO of the metal fragment, an occupied $d_{xy}p_y$ hybrid orbital primarily located at the Ni atom. The trajectory at the C−F bond in the transition state leads to the *cis*-configured product.

Calculations performed on the stationary points of the reaction of octafluoronaphthalene with **1a** or **1b** (see Figure 10) reveal a thermodynamic preference for a coordination of the arene ring at the $\{Ni(^iPr_2Im)_2\}$ complex fragment as it has been observed for the molecular structure of **14** (see Figure 6). The geometry optimized structure of **14** (see Figure 10 bottom left) compares well with the experimental determined molecular structure in the solid state (nickel coordinated at C(19)−C(20), see Figure 6). Isomers with a coordination at C(20)−C(21) or C(19)−C(28) are disfavored by 30.5 and 38.2 kJ/mol, respectively. The calculated bond lengths are Ni−C(1), 1.923 Å (exptl, 1.939(2) Å); Ni−C(10), 1.928 Å (1.941(2) Å); Ni−C(19), 1.989 Å (1.963(2) Å); Ni−C(20), 1.9143 Å (1.886(2) Å); C(19)−C(20), 1.459 Å (1.461(3) Å); F(1)−C(19), 1.391 Å (1.411(2) Å); and F(2)−C(20), 1.392 Å (1.413(2) Å); and angles F(1)−C(19)−Ni, 107.74° (109.04(12)°); and F(2)−C(20)−Ni, 123.13° (125.98(13)°) (for numbering scheme see Figure 6). The dihedral angle between the plane defined by Ni, C(19) and C(20) (see Figure 6) and the plane defined by the naphthalene ligand of the optimized structure is 106.5° (exptl, 108°). The transition states leading to the products of an activation at the 1- or in the 2-position are 114.2 and 106.5 kJ/mol higher in energy with respect to the η^2(C,C) intermediate lowest in energy, which is in good accordance with the activation enthalpy obtained experimentally (116 ± 8 kJ/mol) for this process.

The stationary points on the potential energy surface for the reaction of $[Ni_2(^iPr_2Im)_4(COD)]$ **1a** with C_6H_6 are also summarized in Figure 9 (dotted entries). The most important difference for the activation of C_6H_6 and C_6F_6 can be found in the energetics of the oxidative addition step. First of all, the transfer of the $\{Ni(^iPr_2Im)_2\}$ moiety from **1a** to benzene is endothermic (51.3 kJ/mol), which is in accordance with our observation that we never detected such species. The geometry of the η^2-coordinated intermediate, $[Ni(^iPr_2Im)_2(\eta^2(C,C)\text{-}C_6H_6)]$, is comparable to those described for the fluorinated species, but the Ni−C bonds are slightly longer and the elongation of the coordinated C−C bond as well as the folding of the arene ring is less pronounced. Once formed, cleavage of the C−H bond starting from $[Ni(^iPr_2Im)_2(\eta^2(C,C)\text{-}C_6H_6)]$ is strongly endothermic, with products of the C−H activation lying 22.9 kJ/mol (*trans*) and 45.3 kJ/mol (*cis*) above the η^2 intermediate. The activation barrier for the C−H activation process is significantly smaller (51.0 kJ/mol) compared to barrier for the activation of the C−F bond in hexafluorobenzene. The calculated structure of the transition state is much more productlike than that calculated for the corresponding C−F activation process. This is reflected in the significant increase in the C−H bonding distance (1.565 Å).

Over all, oxidative addition of the C−F bond of C_6F_6 at the nickel fragment $\{Ni(^iPr_2Im)_2\}$ is exothermic, whereas each step of the C−H activation of C_6H_6 is endothermic. Therefore, the nickel system described here is better suited to selective C−F bond activation rather than C−H bond activation mainly because of the strong thermodynamic preference, which starts with the formation of the η^2(C,C) complex.

Our calculations are also in agreement with the experimentally observed chemoselectivity of the activation reactions of partially fluorinated aromatics (*vide supra*). The energies of possible products of the reaction of **1a** with 1,3,5-trifluorobenzene clearly demonstrate a thermodynamic preference for the formation of

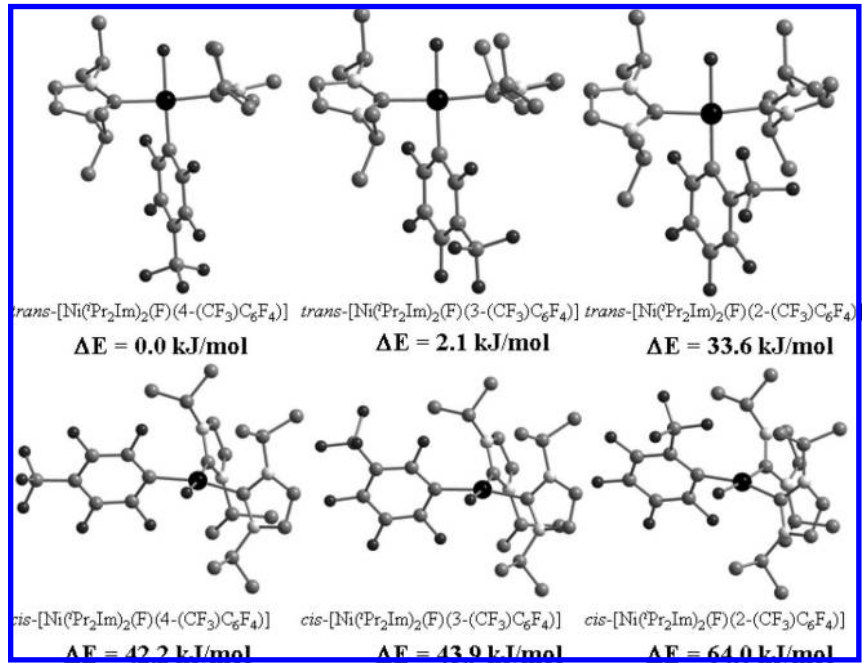

Figure 11. Calculated structures and relative energies of likely activation products of octafluorotoluene with **1a** or **1b**.

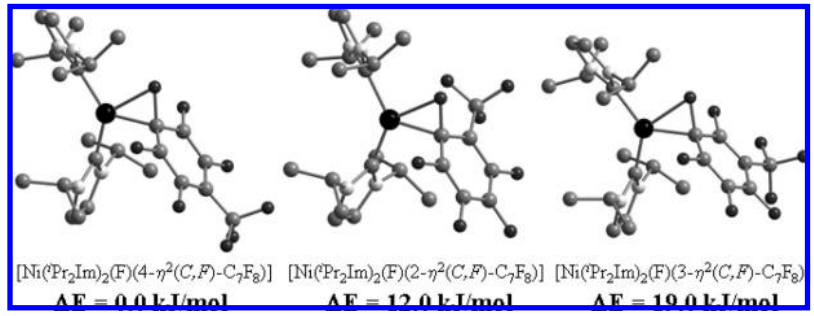

Figure 12. Calculated structures and relative energies of likely transition states of the reaction of octafluorotoluene with **1a** or **1b**.

the experimentally observed C−F activation product *trans*-[Ni(^{i}Pr$_2$Im)$_2$(F)(3,5-C$_6$F$_2$H$_3$)] **8** (see Supporting Information).

The reaction of **1a** with perfluorinated arenes C$_6$F$_5$X (X = H, SiMe$_3$, CF$_3$, C$_6$F$_5$) occurs with a high regioselectivity at the C−F bond in the *para* position to the X group, exemplified by the synthesis and characterization of the complexes *trans*-[Ni(^{i}Pr$_2$Im)$_2$(F)(4-(CF$_3$)C$_6$F$_4$)] **3**, *trans*-[Ni(^{i}Pr$_2$Im)$_2$(F)(4-(C$_6$F$_5$)-C$_6$F$_4$)] **4**, *trans*-[Ni(^{i}Pr$_2$Im)$_2$(F)(4-(SiMe$_3$)C$_6$F$_4$)] **5**, and *trans*-[Ni(^{i}Pr$_2$Im)$_2$(F)(2,3,5,6-C$_6$F$_4$H)] **11**. For a closer examination, DFT calculations have been performed on all possible isomers of a likely C−F activation product of octafluorotoluene. The ground-state energies of all geometry optimized *cis* and *trans* isomers of a C−F activation of C$_7$F$_8$ in the *ortho*, *meta*, and *para* positions of the ring have been calculated as well as the conceivable products of a C−F activation product at the octafluorotoluene CF$_3$ group. These results are summarized in Figure 11, the energies are given with respect to the energy of the experimentally observed complex *trans*-[Ni(^{i}Pr$_2$Im)$_2$(F)(4-(CF$_3$)C$_6$F$_4$)] **3** (= 0 kJ/mol).

These calculations reveal that complexes of the type *cis*-[Ni(^{i}Pr$_2$Im)$_2$(F)((CF$_3$)C$_6$F$_4$)] are in each case much higher in energy with respect to their *trans*-configured counterparts, as it has been found for the activation products of hexafluorobenzene and 1,3,5-trifluorobenzene. Two of the *trans* isomers, *trans*-[Ni(^{i}Pr$_2$Im)$_2$(F)(3-(CF$_3$)C$_6$F$_4$)] and *trans*-[Ni(^{i}Pr$_2$Im)$_2$(F)(4-(CF$_3$)C$_6$F$_4$)], differ only by 2.1 kJ/mol in energy. The third isomer, *trans*-[Ni(^{i}Pr$_2$Im)$_2$(F)(2-(CF$_3$)C$_6$F$_4$)], the reaction product of an activation in the *ortho* position relative of the CF$_3$ group, is 33.6 kJ/mol higher in energy compared to the experimentally observed structure. A closer inspection of a likely η^2(C,C)-bonded intermediate reveals that η^2(C,C) binding of the {Ni(^{i}Pr$_2$Im)$_2$} complex fragment is actually preferred at the 1,2 C−C bond in octafluorotoluene, that is, the bond of the *ipso* carbon atom at the CF$_3$ substituent to the *ortho* carbon atom. The product of a coordination at the 2,3 C−C bond is disfavored by 11.3 kJ/mol, at the 3,4 C−C bond by 4.8 kJ/mol. However, if we presume that these isomers are in rapid equilibrium to each other, the different energies of the 1,2 C−C and 3,4 C−C η^2-intermediates will have no influence on the selectivity of the product formation (Curtin−Hammett principle).

Relative energies and structures of the optimized transition states are given in Figure 12. For a concerted oxidative addition, these relative energies reveal a kinetic preference for the formation of *trans*-[Ni(^{i}Pr$_2$Im)$_2$(F)(4-(CF$_3$)C$_6$F$_4$)] **3**, because the transition state corresponding to this complex is favored by 12.0 kJ/mol with respect to the transition state resulting for an activation of the *ortho* fluorine atom and 19.0 kJ/mol with respect to the transition state resulting for an activation of the *meta* fluorine atom.

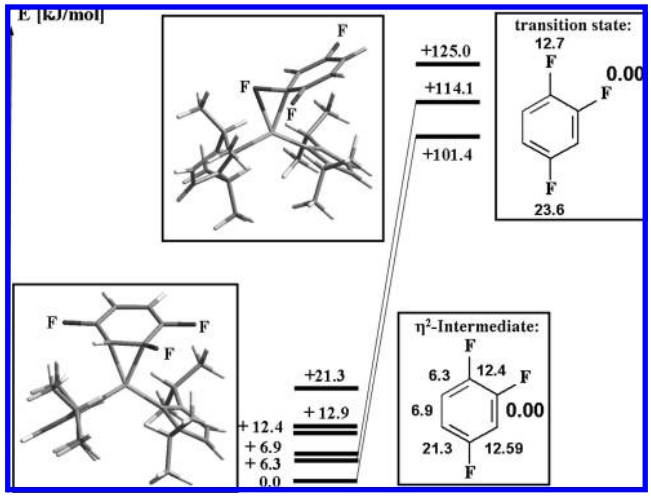

Figure 13. Relative energies of all possible η^2 intermediates and likely transition states of the reaction of 1,2,4-trifluorobenzene with **1a** or **1b**. The optimized structures of the η^2 intermediate of lowest energy and the transition state of lowest energy are given.

The reactions of **1a** with the partially fluorinated aromatic substrates 1,2,3-$C_6H_3F_3$ and 1,2,4-$C_6H_3F_3$ pose the interesting question about the relative stability of the possible isomeric C−F activation products. In the case of 1,2,4-trifluorobenzene, the C−F activation product *trans*-[Ni(^{i}Pr$_2$Im)$_2$(F)(2,5-$C_6F_2H_3$)] **10** was the only isomer observed. The results of our calculations on the relative stabilities of all possible η^2-bonded intermediates and the likely transition states of C−F activation are summarized in Figure 13. All possible η^2-(C,C) intermediates have been optimized. There is no clear trend for a preference of {Ni(^{i}Pr$_2$Im)$_2$} coordination which might be deduced from simple fluorine substituent positioning arguments. We calculate a preference for the coordination of {Ni(^{i}Pr$_2$Im)$_2$} in the 2,3 C−C position, followed by a coordination at the 1,6 (+6.3 kJ/mol) and the 5,6 (+6.9 kJ/mol) positions. Coordination at the 5,6 C−C bond is unproductive for C−F activation, but coordination at the other two positions may lead to C−F activation. An examination of all three transition states reveal that the transition state for an activation in the 2 position is 101.4 kJ/mol above the η^2 intermediate of lowest energy. Relative to this transition state are the transition states for C−F activation in the 1 or 4 position, 12.7 and 23.6 kJ/mol higher in energy, respectively. Therefore, the relative stabilities of the η^2 bonded intermediates as well as the relative energies of the transition states of the C−F activation nicely reflect the experimental results.

In case of the reaction of **1a** with 1,2,3-trifluorobenzene at −78 °C we observe experimentally a mixture of the isomers *trans*-[Ni(^{i}Pr$_2$Im)$_2$(F)(2,3-$C_6F_2H_3$)] **9a** (approximately 85% judged by ^{19}F NMR spectroscopy) and *trans*-[Ni(^{i}Pr$_2$Im)$_2$(F)(2,6-$C_6F_2H_3$)] **9b** (approximately 15% judged by ^{19}F NMR spectroscopy); that is, the activation product of the statistically more favored C−F bonds in the 1 position is the major isomer. All possible η^2-(C,C) intermediates have been optimized and those in which the nickel atom is coordinated in 1,2, 2,3, 3,4, and 6,1 positions are very close in energy. The energetic difference between coordination at these positions is a mere 0.1 kJ/mol. Statistically, η^2 intermediates with {Ni(^{i}Pr$_2$Im)$_2$} at the 1,2 and 2,3 position would each lead to 50% insertion into the C−F bond at 1(3) position and at 2 position, whereas complexes with nickel attached to the 6,1 or 3,4 bond would lead to 100% insertion into the C−F bond at the 1(3) position. Therefore, a distribution of 25% activation of the C−F bond in the 2 position and 75% activation of the C−F bond in the 1(3) position is expected by statistical means. This scheme has to be altered in dependence of the relative energies of the transition states. In this case, however, we calculate the lowest energy transition state for the η^2-(C,F) complex leading to the activation product in the 2-position, which contradicts our experimental findings. This transition state lies 87.2 kJ/mol above the η^2-(C,C) intermediate of lowest energy and is actually the lowest barrier we have calculated for all the cases considered here (C_6F_6, 101.5 kJ/mol; $C_{10}F_8$, 106.5 kJ/mol; C_7F_8, 90.9 kJ/mol; 1,2,4-$C_6H_3F_3$, 101.4 kJ/mol).

Discussion

The C−F activation of polyfluorinated arenes as depicted in Scheme 1 and Scheme 2 proceeds smoothly using the complexes [Ni$_2$(^{i}Pr$_2$Im)$_4$(COD)] **1a** or [Ni(^{i}Pr$_2$Im)$_2$(η^2-C_2H_4)] **1b**, which serve as a readily available source of the {Ni(^{i}Pr$_2$Im)$_2$} complex fragment. As it has been found for nickel phosphine compounds, these activation reactions show a high chemoselectivity for the activation of the C−F bond over the C−H bond. This is in contrast to a variety of other C−F activation reactions (e.g., at Ru, Rh, or Re), which exhibit a preference for C−H activation over C−F activation.[1f,i,2i,5g] A nickel fluorobenzyne complex has shown to react via C−H activation rather than C−F activation.[24] At {Ni(^{i}Pr$_2$Im)$_2$} partially fluorinated aromatics and polyfluorinated aromatics of the type C_6F_5X such as octafluorotoluene (X = CF_3), trimethyl(pentafluorophenyl)silane (X = $SiMe_3$), decafluorobiphenyl (X = C_6F_5), and pentafluorobenzene (X = H) are activated regioselectively in the *para* position to the X group. Our DFT calculations, which are in good agreement with the experiment, give a more detailed insight into the observed chemo- and regioselectivities of this reaction.

Interestingly, the reaction of **1a** and **1b** with pentafluoropyridine performed at low temperatures afforded *trans*-[Ni(^{i}Pr$_2$Im)$_2$(F)(4-C_5NF_4)] **12a** as the sole product of the reaction. A reaction of **1b** at room temperature led to the formation of a mixture of *trans*-[Ni(^{i}Pr$_2$Im)$_2$(F)(4-C_5NF_4)] **12a** and *trans*-[Ni(^{i}Pr$_2$Im)$_2$(F)(2-C_5NF_4)] **12b** in a ratio of 1:2. Previous studies on the reaction of pentafluoropyridine with transition metal complexes have shown that nickel complexes tend to activate at the 2-position, whereas carbon−fluorine bond activation reactions using platinum or palladium complexes led to an activation at the 4 position.[5a,2i,17]

In the case of hexafluorobenzene and octafluoronaphthalene we were able to identify the η^2(C,C)-bonded intermediates [Ni(^{i}Pr$_2$Im)$_2$(η^2-C_6F_6)] **13** and [Ni(^{i}Pr$_2$Im)$_2$(η^2-$C_{10}F_8$)] **14** by NMR spectroscopy as well as X-ray crystallography in the case of the octafluoronaphtalene complex. Both compounds exhibit a coordination of the aromatic system in an η^2-fashion. The NMR data at variable temperature indicate a dynamic behavior for both complexes, which arises presumably from suprafacial 1,3-shifts. These observation are in accordance with the dynamic behavior of [Ni{^{t}Bu$_2$P(CH$_2$)$_2$P^{t}Bu$_2$}(η^6-C_6F_6)] found earlier, which is maintained in solution even at low temperatures.[9] The coordination of octafluoronaphthalene at {Ni(PEt$_3$)$_2$} also leads to an η^2-complex, which is also highly fluxional.[10]

The activation enthalpy for the rearrangement of **14** into the C−F activation products **6a** and **6b** has been monitored in d_8 toluene by ^{19}F NMR spectroscopy at different temperatures. The

(24) (a) Keen, A. L.; Johnson, S. A. *J. Am. Chem. Soc.* **2006**, *128*, 1806. (b) Keen, A. L.; Doster, M.; Johnson, S. A. *J. Am. Chem. Soc.* **2007**, *129*, 810.

rate constants are first order. The activation enthalpy according to the Eyring equation gave an estimation of $\Delta H^{\ddagger}$ of 116 ± 8 kJ/mol. To our knowledge, this is one of the few known experimental estimations for the kinetic barrier of an oxidative addition reaction of a C−F bond. Note that kinetic studies by Crespo et al. led to activation enthalpies for the cyclometalation of fluorinated imines at platinum centers of $\Delta H^{\ddagger} = 30-54$ kJ/mol.[25] Furthermore, the (solution) kinetic data for the conversion of **14** to **6a/6b** are compatible with our (gas phase) calculations at {Ni(^{i}Pr$_2$Im)$_2$}.

Our results from the kinetic studies can also be compared with data from theoretical investigations for group 9 and 10 metals. For the oxidative addition of fluorobenzene at {Pd(PH$_3$)$_2$} the activation enthalpy has been calculated to be $\Delta H^{\ddagger} = 172.5$ kJ/mol,[7b] and for the rearrangement of [Rh(η^2-C$_6$F$_6$)(η^5-C$_5$Me$_5$)(PMe$_3$)] into [Rh(F)(C$_6$F$_5$)(η^5-C$_5$Me$_5$)(PMe$_3$)] an activation enthalpy of $\Delta H^{\ddagger} = 139.4$ kJ/mol has been calculated for the C−F bond cleavage.[6b] Perutz and McGrady studied the activation of C$_6$F$_6$ and C$_6$H$_6$ as model substrates at nickel and platinum.[6a] The studies suggest the reaction to occur via a concerted oxidative addition mechanism. Carbon−fluorine bond cleavage by [M{H$_2$P(CH$_2$)$_2$PH$_2$}] (M = Ni, Pt) is thermodynamically favorable, but in case of the platinum compound the oxidative addition is kinetically more hampered due to an activation barrier of $\Delta H^{\ddagger} = 122.7$ kJ/mol compared to the nickel fragment ($\Delta H^{\ddagger} = 94.2$ kJ/mol). The reaction pathway at the zerovalent nickel complex fragment [Ni(H$_2$PCH$_2$CH$_2$PH$_2$)] was calculated to proceed via an initial formation of an η^2-coordinated arene complex. Two distinct transition states have been located on the potential energy surface between the η^2-coordinated arene and the oxidative addition product. The first one features a η^3-coordinated arene ligand and connects two identical η^2-arene minima, whereas the other transition state, an η^2-(C,F)-σ complex, leads to the cleavage of the C−F bond. The resulting product of the C−F activation reaction, [Ni(H$_2$PCH$_2$CH$_2$PH$_2$)(F)(C$_6$F$_5$)], was predicted to be 82.4 kJ/mol lower in energy with respect to the η^2-coordinated intermediate. Our DFT calculations on carbene and on nonchelating phosphine systems also reveal that there is a strong thermodynamic driving force for C−F bond cleavage using Ni(0) complexes.

A conceivable reaction pathway for the C−F activation reactions thus consists of a precoordination of the substrate at the nickel bis(carbene) complex fragment followed by the oxidative addition via a concerted mechanism. Our experimental data presented here in combination with DFT calculations overall agree with such a mechanism. We detected or isolated complexes with η^2-(C,C)-coordinated hexafluorobenzene and octafluoronaphthalene ligands. The rates for the disappearance of **14** to form the products of the oxidative addition follow first order kinetics and the experimentally deduced activation barriers are compatible with our calculations at {Ni(^{i}Pr$_2$Im)$_2$}.

Note that alternative reaction pathways for the C−F activation step have also been discussed.[1,2i,5,26] They proceed via an electron transfer to give a tight ion pair as the key intermediate or comprise a nucleophilic substitution. The latter pathway is initiated by nucleophilic attack of the metal at the electrophilic site of the aromatic system usually as the rate-determining step.[27] In this case a precoordination of the fluorinated substrate might also play a crucial role, before charge separation occurs.

However, the question remains *why* the NHC stabilized systems such as [Ni$_2$(^{i}Pr$_2$Im)$_4$(COD)] **1a** and [Ni(^{i}Pr$_2$Im)$_2$(η^2-C$_2$H$_4$)] **1b** are faster for the C−F activation of perfluorinated benzenes in comparison to the corresponding phosphine complexes. Perutz et al. reported that the reaction of hexafluorobenzene with [Ni(COD)$_2$] in the presence of triethylphosphine or with [Ni(PEt$_3$)$_4$] at room temperature results in very slow formation of *trans*-[Ni(PEt$_3$)$_2$(F)(C$_6$F$_5$)], taking four weeks to reach completeness.[2h,5f] According to our calculations in the gas phase the barrier should be comparable for an concerted oxidative addition at {Ni(^{i}Pr$_2$Im)$_2$} or {Ni(PEt$_3$)$_2$} (101.5 and 111.4 kJ/mol, respectively). Thus the data for {Ni(PEt$_3$)$_2$} do not agree with reaction times, which have been found in the experiment.

Taking the rapid reaction of the {Ni(^{i}Pr$_2$Im)$_2$} system and its high nucleophilicity into account, it has to be considered that the concerted oxidative addition of a carbon−fluorine bond is characterized by a considerable contribution of a nucleophilic attack of the basic {Ni(^{i}Pr$_2$Im)$_2$} fragment at the C−F bond; that is, a charge separation might play a certain role resulting in a faster reaction. This suggestion might be corroborated by the addition of pentafluoropyridine to {Ni(^{i}Pr$_2$Im)$_2$}, which leads at low temperatures to an activation at the 4-position yielding *trans*-[Ni(^{i}Pr$_2$Im)$_2$(F)(4-C$_5$NF$_4$)] **12a**, whereas at room temperature a reaction of {Ni(^{i}Pr$_2$Im)$_2$} gives **12a** and *trans*-[Ni(^{i}Pr$_2$Im)$_2$(F)(2-C$_5$NF$_4$)] **12b**. Note that the 4-position in pentafluoropyridine is the position susceptible for a nucleophilic attack. In contrast, treatment of [Ni(COD)$_2$] with pentafluoropyridine in the presence of PEt$_3$ results in the formation of complex *trans*-[Ni(PEt$_3$)$_2$(F)(2-C$_5$NF$_4$)].[5f] Notably, C−F bond activation reactions using basic Pt, Pd, and Rh complexes also led to an activation at the 4-position.[5a,2i,17]

Conclusions

We presented a combined experimental and theoretical study on carbon−fluorine bond activations at {Ni(^{i}Pr$_2$Im)$_2$}. The reactions proceed very fast and are highly regio- and chemoselective. Mechanistic studies on the activation of hexafluorobenzene and octafluoronaphthalene led to the detection of intermediates with the aromatic system coordinated in an η^2-fashion. First order kinetics have been obtained for the oxidative addition of the octafluoronaphthalene unit at the nickel center leading to an estimated $\Delta H^{\ddagger}$ of 116 ± 8 kJ/mol. DFT calculations are in accordance with this activation barrier, but also with the regio- and chemoselectivities, which have been found experimentally. For the mechanisms of the C−F activation step we suggest a

(25) Crespo, M.; Martínez, M.; de Pablo, E. J. *Dalton Trans.* **1997**, 1231.
(26) Noveski, D.; Braun, T.; Schulte, M.; Neumann, B.; Stammler, H.-G. *Dalton Trans.* **2003**, 4075.
(27) Beletskaya, I. P.; Artamkina, G. A.; Mil'chenko, A. Y.; Sazonov, P. K.; Shtem, M. M. *J. Phys. Org. Chem.* **1996**, *9*, 319.
(28) (a) Ahlrichs, R.; Bär, M.; Häser, M.; Horn, H.; Kölmel, C. *Chem. Phys. Lett.* **1989**, *162*, 165. (b) Häser, M.; Ahlrichs, R. *J. Comput. Chem.* **1989**, *10*, 104. (c) von Arnim, M.; Ahlrichs, R. *J. Comput. Chem.* **1998**, *19*, 1746.
(29) (a) Becke, A. D. *Phys. Rev. A* **1988**, *38*, 3098. (b) Perdew, J. P. *Phys. Rev. B* **1986**, *33*, 8822; (erratum) Perdew, J. P. *Phys. Rev. B* **1986**, *34*, 7406.
(30) (a) Treutler, O.; Ahlrichs, R. *J. Chem. Phys.* **1995**, *102*, 346. (b) Eichkorn, K.; Treutler, O.; Öhm, O.; Häser, M.; Ahlrichs, R. *Chem. Phys. Lett.* **1995**, *240*, 283. (c) Eichkorn, K.; Weigend, F.; Treutler, O.; Ahlrichs, R. *Theor. Chem. Acc.* **1997**, *97*, 119.
(31) (a) Eichkorn, K.; Treutler, O.; Öhm, H.; Häser, M.; Ahlrichs, R. *Chem. Phys. Lett.* **1995**, *242*, 652. (b) Haase, F.; Ahlrichs, R. *J. Comput. Chem.* **1993**, *14*, 907. (c) Weigand, F.; Häser, M. *Theor. Chem. Acc.* **1997**, *97*, 331. (d) Weigand, F.; Häser, M.; Patzelt, H.; Ahlrichs, R. *Chem. Phys. Lett.* **1998**, *294*, 143.
(32) Schäfer, A.; Horn, H.; Ahlrichs, R. *J. Chem. Phys.* **1992**, *97*, 2571.
(33) de Jong, G. T.; Bickelhaupt, F. M. *J. Phys. Chem. A* **2005**, *109*, 9685.

precoordination of the aromatic system prior to a concerted oxidative addition. The latter might be facilitated by the nucleophilicity of the $\{Ni(^{i}Pr_2Im)_2\}$ fragment.

(34) (a) Sheldrick, G. M. *SHELXS-97, Program for Crystal Structure Solution;* Universität Göttingen: Göttingen, Germany, 1997. (b) Sheldrick, G. M. *SHELXL-97, Program for Crystal Structure Refinement*; Universität Göttingen: Göttingen, Germany, 1997. (c) *SHELXTL-PLUS*; Siemens Analytical X-Ray Instruments Inc.: Madison, WI, 1990.

Acknowledgment. We are grateful for financial support of the Universität Karlsruhe (TH), the Fonds der Chemischen Industrie, and the Deutsche Forschungsgemeinschaft.

Supporting Information Available: X-ray crystal data in CIF format, experimental and computational details. The CCDC numbers for the CIFs are 651595−651597. This material is available free of charge via the Internet at http://pubs.acs.org.

JA074640E